

Chip-Interleaved Block-Spread CDMA Versus DS-CDMA for Cellular Downlink: A Comparative Study

Shengli Zhou, *Member, IEEE*, Pengfei Xia, *Student Member, IEEE*, Geert Leus, *Member, IEEE*, and Georgios B. Giannakis, *Fellow, IEEE*

Abstract—A so-termed chip-interleaved block-spread (CIBS) code division multiple access (CDMA) system has been introduced for cellular applications in the presence of frequency selective multipath channels. In both uplink and downlink operation, CIBS-CDMA achieves multiuser-interference (MUI) free reception within each cell. This paper focuses on the cellular downlink configuration and compares CIBS-CDMA against the conventional direct-sequence (DS) CDMA system, which relies on a chip equalizer to restore code orthogonality and, subsequently, suppresses MUI by despreading. We provide a unifying framework for both systems and investigate their performance in the presence of intercell interference and soft-handoff operation. Extensive comparisons from load, performance, complexity, and flexibility perspectives illustrate the merits, along with the disadvantages, of CIBS-CDMA over DS-CDMA, and reveal its potential for future wireless systems.

Index Terms—Code division multiple access (CDMA), cellular downlink, frequency-selective channel, multiuser interference (MUI).

I. INTRODUCTION

RELYING on orthogonal spreading codes, code division multiple access (CDMA) enables simultaneous transmissions from multiple users over the same time-bandwidth slot. However, as the chip rate increases in high-rate wireless applications, the underlying multipath channels become time dispersive and introduce frequency selective effects. Although the frequency-selective multipath channels introduce multipath diversity, which can be collected by a RAKE receiver, they also cause interchip interference (ICI) which destroys code orthogonality at the receiver. The latter gives rise to multiuser interfer-

ence (MUI) and severely limits the performance of single user RAKE receivers in a multiuser setting. To suppress MUI, various linear or nonlinear multiuser detectors have been proposed [20]. However, these schemes are more suitable for uplink transmissions, where the base station (BS) has knowledge of the multipath channels and spreading codes of all users and is thus able to demodulate all users' information either jointly or separately.

In this paper, we focus on downlink CDMA that presents some distinct challenges and characteristics relative to its uplink counterpart. First, downlink transmissions come with symbol-aperiodic spreading, where each user's information symbols are spread by a short user-specific code and then scrambled by a long BS-specific code. Second, the chip sequences of all users are multiplexed in a synchronous fashion before transmission. The signals of all users thus experience a single propagation channel to reach each particular mobile station (MS). Finally, each MS only needs to demodulate its own data and, generally, does not know the spreading codes of other users.

Accounting for these unique downlink features, a class of linear receivers with chip equalization has been developed to suppress MUI in downlink direct sequence (DS)-CDMA [2], [3], [6], [7], [9], [10]. These receivers share the simple but elegant idea of first linearly equalizing the frequency-selective channel to restore completely, or partially, the multiuser signal transmitted from the BS at the chip rate and then correlating the resulting chip sequence with the spreading code to decode the information of the desired user. DS-CDMA receivers equipped with zero forcing (ZF) or minimum mean square error (MMSE) chip equalizers have been shown to offer significant performance gains over the conventional RAKE receiver [2], [3], [7], [9].

Recently, transceiver designs have been proposed which remove MUI deterministically, regardless of the underlying multipath channels, and are applicable to both uplink and downlink operations. Those include the orthogonal frequency division multiple access (OFDMA) [17], the generalized multicarrier (GMC) CDMA [4], [22], the shift-orthogonal CDMA [11], and the chip-interleaved block-spread (CIBS) CDMA [23]. The comparisons among MUI-free transceivers favor CIBS-CDMA [23], which constitutes the focus of this paper.

The CIBS-CDMA transceiver is depicted in [23, Fig. 4]. Compared to the conventional DS-CDMA, the CIBS-CDMA transmitter block interleaves the chip sequence obtained by symbol spreading and inserts guard intervals before its transmission. At the receiver, the received samples are deinterleaved

Manuscript received February 7, 2002, revised September 9, 2002; accepted November 12, 2002. The editor coordinating the review of this paper and approving it for publication is Q. Bi. This work was supported in part by the ARL/CTA under Grant DAAD19-01-2-011 and by the National Science Foundation under Grant 0105612. This paper was presented in part at the International Conference on Acoustics, Speech, and Signal Processing (ICASSP), Orlando, FL, May 2002, and at the International Conference on Circuits and Systems (ISCAS), Scottsdale, AZ, May 2002.

S. Zhou was with the Department of Electrical and Computer Engineering, University of Minnesota, Minneapolis, MN 55455 USA. He is now with the Department of Electrical and Computer Engineering, University of Connecticut, Storrs, CT 06269 USA (e-mail: shengli@enr.uconn.edu).

P. Xia, and G. B. Giannakis are with the Department of Electrical and Computer Engineering, University of Minnesota, Minneapolis, MN 55455 USA (e-mail: pfxia@ece.umn.edu; georgios@ece.umn.edu).

G. Leus is with the Faculty of Electrical Engineering, Mathematics and Computer Science, Delft University of Technology, 2628 CD Delft, The Netherlands (e-mail: leus@cas.et.tudelft.nl).

Digital Object Identifier 10.1109/TWC.2003.821166

and correlated with each user’s spreading (or signature) code. Thanks to the judicious transmitter design, CIBS-CDMA maintains code orthogonality among different users even after frequency selective propagation, which enables deterministic MUI-free reception through low-complexity code-matched filtering (or correlation). However, only one cell is considered in [23].

In this paper, we compare downlink CIBS-CDMA against the downlink DS-CDMA system equipped with chip equalization at the receiver. We first provide a unifying framework for both systems and then investigate their performance in the presence of intercell interference and under soft-handoff operations. Extensive comparisons from load, performance, complexity, and flexibility perspectives suggest the following interesting results.

- 1) The maximum number of users in DS-CDMA is slightly higher than that in CIBS-CDMA. This is the price paid by CIBS-CDMA for MUI-free reception within each cell due to the redundancy introduced by guard intervals.
- 2) CIBS-CDMA is more flexible than DS-CDMA when it comes to equalization. Nonlinear receivers with high performance and moderate complexity can be deployed in CIBS-CDMA, exploiting the finite alphabet property of user symbols. Lack of other users’ decoded symbols prevents the use of these nonlinear receivers for downlink DS-CDMA.
- 3) With linear MMSE equalizers and without handoff, CIBS-CDMA has performance comparable to DS-CDMA with high system load and is inferior to DS-CDMA with low system load. However, CIBS-CDMA has better performance than DS-CDMA when handoff operation is accounted for. Nonlinear equalizers boost the performance of CIBS-CDMA and yield a clear advantage over DS-CDMA.
- 4) With linear equalizers, CIBS-CDMA involves lower equalization and despreading complexity than DS-CDMA, although the relative complexity for constructing the equalizer depends on the chosen system parameters.
- 5) In CIBS-CDMA, power control can be used effectively, since multiple users are decoupled.

The rest of the paper is organized as follows: Section II presents the system model for both systems. Section III investigates intercell interference and analyzes performance. Section IV is devoted to soft handoff, and Section V details further comparisons between these two downlink systems. Simulation results are collected in Section VI, while conclusions are drawn in Section VII.

Notation: Bold upper-case letters denote matrices, and bold lower-case letters stand for column vectors; $(\cdot)^T$, $(\cdot)^H$, and $(\cdot)^\dagger$ denote transpose, Hermitian transpose, and pseudoinverse, respectively; \otimes denotes the Kronecker product, and $\delta[\cdot]$ denotes the Kronecker delta; $E\{\cdot\}$ stands for ensemble expectation; \mathbf{I}_K denotes the $K \times K$ identity matrix, and $\mathbf{0}_{M \times N}$ denotes the $M \times N$ all zero matrix; $[\cdot]_p$ stands for the $(p + 1)$ st entry of a vector, and $[\cdot]_{p,q}$ stands for the $(p + 1, q + 1)$ st element of a matrix. Throughout this paper, k is used to index symbols, n for chips, and u for users.

II. SYSTEM MODEL

In this section, we present the downlink transceiver model for both DS-CDMA and CIBS-CDMA systems. To allow for a fair comparison, we unify these two systems on a frame level, where users transmit in a frame-by-frame fashion. Notice that one frame here corresponds to one time slot in time-division (TD) CDMA-based UMTS terrestrial radio access (UTRA) time-division duplex (TDD) mode [5]. During each frame, we assume that the number of active users U is constant, and the channels remain invariant. Channel estimation is performed once per frame or once per time slot as detailed in [5]. We assume that the channel estimates are perfect at the receiver. The impact of channel variation and imperfect channel estimation on system performance is certainly an important issue, but beyond the scope of this paper.

A. Unifying Model Per Frame

Each user transmits K_f information symbols per frame that we collect in the vector $\mathbf{s}_u := [s_u[0], \dots, s_u[K_f - 1]]^T$, where $u \in \{1, \dots, U\}$. With T_c denoting the chip interval, and T_f the frame interval, each frame contains $N_f := T_f/T_c$ chips. Assuming linear modulation, the information block \mathbf{s}_u is first spread to form an $N_f \times 1$ chip block $\mathbf{x}_u := \mathbf{C}_u \mathbf{s}_u$, where \mathbf{C}_u denotes the $N_f \times K_f$ spreading matrix of user u . The difference between downlink DS-CDMA and downlink CIBS-CDMA boils down to different designs of the matrix \mathbf{C}_u . For synchronous transmissions, the BS sums all users’ chip sequences to obtain

$$\mathbf{x} := \sum_{u=1}^U A_u \mathbf{x}_u = \sum_{u=1}^U A_u \mathbf{C}_u \mathbf{s}_u \quad (1)$$

where the weight A_u is introduced to control the u th user’s transmit power. The multiuser chip sequence $x[n]$ corresponding to \mathbf{x} is then passed through the pulse-shaping filter, modulated to a high carrier frequency, and transmitted.

At the receiver, we allow for multichannel reception which becomes available, for example, by sampling the received signal at rate M_s/T_c , where $M_s \geq 1$ denotes the oversampling factor. Alternatively, multiple receive antennas¹ can be deployed at the mobile to boost system performance, as proposed for downlink DS-CDMA in [9]. Due to size limitations, the mobile can often deploy up to $M_r = 2$ receive antennas. Both oversampling and multiantenna reception create multiple channels. In general, multiantenna reception yields independent channels, while oversampling generally results in dependent channels, which makes a difference in performance. But for now, we will not differentiate between these two cases. Supposing each receive antenna is oversampled by M_s , we consider a system with $M = M_r M_s$ effective channels (and thus receivers). This includes single-antenna reception with no oversampling as a special case corresponding to $M = M_r = M_s = 1$.

Denote with $\mathbf{h}_m := [h_m[0], \dots, h_m[L]]^T$ the discrete-time base-band equivalent channel between the transmitter and the m th ($m \in \{1, 2, \dots, M\}$) receiver, where L is an upper bound

¹Another way could be to deploy polarization diversity [19].

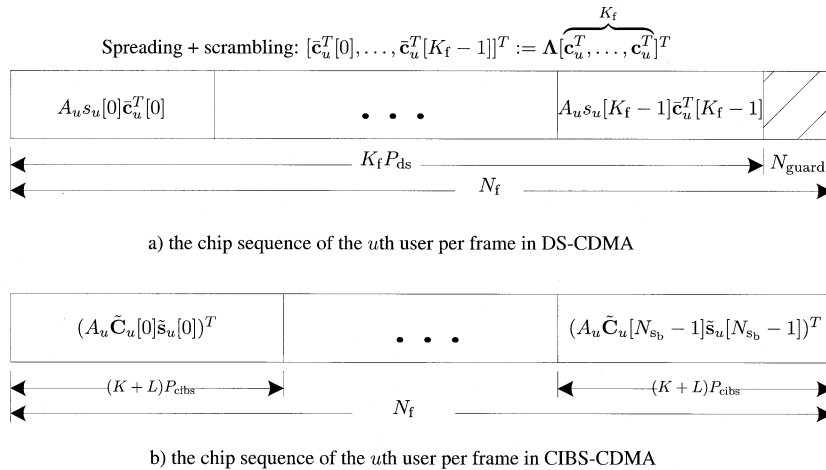


Fig. 1. Frame structure for DS-CDMA and CIBS-CDMA systems.

on the channel order. This equivalent channel includes the physical channel as well as transmit and receive filters. Let $\tau_{s,\max}$ be the maximum channel delay spread and T_{support} the nonzero support of the filter obtained by linearly convolving the transmit with the receive filter. Usually, the overall channel order L is overestimated as $L = \lceil (\tau_{s,\max} + T_{\text{support}} + \tau_{\text{margin}}) / T_c \rceil$; the usefulness of τ_{margin} will be explained in Section III when multiple cells are considered.

The received sequence at the m th output can, thus, be written as $y_m[n] = \sum_{l=0}^L h_m[l]x[n-l] + e_m[n]$, where $e_m[n]$ is the additive channel noise that also includes the intercell interference from nearby BSs. If the mobile is far away from the edge of its cell, the intercell interference can be ignored, and $e_m[n]$ reduces to the ambient additive white Gaussian noise (AWGN).

Collecting received chip samples into the $N_f \times 1$ vector $\mathbf{y}_m := [y_m[0], \dots, y_m[N_f - 1]]^T$, and because $N_f \geq L$ can be assured by design, we obtain the following block model for the m th output:

$$\mathbf{y}_m = \mathbf{H}_m \mathbf{x} + \mathbf{H}_m^{(1)} \mathbf{x}^{(1)} + \mathbf{e}_m \quad (2)$$

where \mathbf{e}_m is defined similar to \mathbf{y}_m , \mathbf{H}_m is the lower triangular $N_f \times N_f$ Toeplitz matrix with $[\mathbf{H}_m]_{p,q} = h_m[p - q]$, $\mathbf{H}_m^{(1)}$ is the upper triangular $N_f \times N_f$ Toeplitz matrix with $[\mathbf{H}_m^{(1)}]_{p,q} = h_m[p - q + N_f]$, and $\mathbf{x}^{(1)}$ denotes the previous frame. The term $\mathbf{H}_m^{(1)} \mathbf{x}^{(1)}$ accounts for the interference between adjacent frames and can be easily avoided by introducing a guard interval between successive frames, as it is done in both downlink DS-CDMA and CIBS-CDMA systems. Therefore, (2) can be simplified to

$$\mathbf{y}_m = \mathbf{H}_m \mathbf{x} + \mathbf{e}_m, \quad \forall m = 1, \dots, M. \quad (3)$$

Starting from (3), we next describe the transceivers for DS-CDMA and CIBS-CDMA.

B. Downlink DS-CDMA With Chip Equalization

Conventional DS-CDMA relies on *symbol* spreading. Each user is assigned a distinct $P_{ds} \times 1$ spreading code \mathbf{c}_u , and the spreading codes are designed to be mutually orthonormal, i.e.,

$\mathbf{c}_u^H \mathbf{c}_{u'} = \delta[u - u']$. All chips of the code \mathbf{c}_u have amplitude $1/\sqrt{P_{ds}}$. Each *symbol* $s_u[k]$ is spread by \mathbf{c}_u to yield P_{ds} chips that comprise the vector $\mathbf{c}_u s_u[k]$. The chips corresponding to K_f information symbols are concatenated to form a frame that is scrambled by a BS-specific overlay (long scrambling) code and padded by N_{guard} guard zeros to avoid interframe interference. The resulting sequence comprises the transmitted chips \mathbf{x}_u corresponding to the user u , as depicted in the upper part of Fig. 1. The operations that yield \mathbf{x}_u from \mathbf{s}_u can be captured by designing \mathbf{C}_u in (1) as

$$\mathbf{C}_u = \mathbf{T}_{ds} \mathbf{D}_u, \quad \text{with } \mathbf{D}_u = \mathbf{A}(\mathbf{I}_{K_f} \otimes \mathbf{c}_u) \quad (4)$$

where $\mathbf{T}_{ds} := [\mathbf{I}_{K_f P_{ds}}, \mathbf{0}_{K_f P_{ds} \times N_{\text{guard}}}]^T$ describes the guard inserting operation and \mathbf{A} is a $K_f P_{ds} \times K_f P_{ds}$ diagonal matrix holding on its diagonal the scrambling code with each chip having unit amplitude. Notice that the scrambling matrix \mathbf{A} changes from frame to frame but is identical for all users in the same cell. Different scrambling codes are deployed in different cells for cell identification and intercell-interference suppression purposes. Accounting for the guard, the number of chips per transmitted frame is: $N_f = K_f P_{ds} + N_{\text{guard}}$.

Introducing the guard chips in DS-CDMA avoids interframe interference and allows us to cast both DS-CDMA and CIBS-CDMA under the unifying model (3). We will also find it convenient to define the $K_f P_{ds} \times 1$ chip block $\mathbf{z}_u := \mathbf{D}_u \mathbf{s}_u$ without the guard chips. The corresponding $K_f P_{ds} \times 1$ multiuser chip block is thus

$$\mathbf{z} := \sum_{u=1}^U A_u \mathbf{z}_u = \sum_{u=1}^U A_u \mathbf{D}_u \mathbf{s}_u. \quad (5)$$

Notice that mutual orthogonality among users is also ensured at the frame level since $\mathbf{D}_u^H \mathbf{D}_{u'} = \delta[u - u'] \mathbf{I}_{K_f}$. Hence, for each user u , we obtain $\mathbf{s}_u = (1/A_u) \mathbf{D}_u^H \mathbf{z}$ simply by despreading (5). Based on this observation, if one can extract from $\{\mathbf{y}_m\}_{m=1}^M$ the chip block that we denote as $\hat{\mathbf{z}}$, then for the desired user μ , an estimate of the symbol vector \mathbf{s}_μ can be constructed as

$$\hat{\mathbf{s}}_\mu = \frac{1}{A_\mu} \mathbf{D}_\mu^H \hat{\mathbf{z}} \quad (6)$$

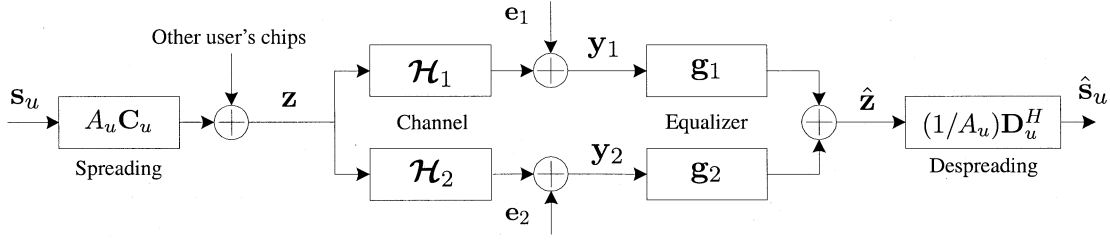


Fig. 2. Transceiver model of DS-CDMA using chip equalizers.

where only knowledge of the desired user's code is required. This kind of DS-CDMA reception requires channel equalization to recover the transmitted chip sequence and then despreading the estimated chip sequence to suppress MUI, hence the name chip equalizer receiver. Notice that symbol-level receivers, which estimate \hat{s}_μ directly from $\{\mathbf{y}_m\}_{m=1}^M$ are also possible [8], [9], [20]; but, they are highly complex in the downlink setup, since the mobile lacks knowledge of other users' codes. More important, the symbol-level detector should change from symbol to symbol to account for the random scrambling [9].

Given $\{\mathbf{y}_m\}_{m=1}^M$, we will invoke chip-level equalization to obtain $\hat{\mathbf{z}}$. Block equalization by inverting the matrix \mathbf{H}_m in (3) is certainly possible [7], but computationally prohibitive, since the frame size N_f is large, in general. We, here, only consider the practical approach developed in [3], [6], [9], [10], and [15] that relies on serial equalizers. A transceiver diagram is depicted in Fig. 2.

With $\{g_m[l]\}_{l=0}^{L_g}$ denoting the L_g th order chip equalizer for the m th antenna, the receiver estimates the chip sequence as: $\hat{z}[n - D] = \sum_{m=1}^M g_m[n] * y_m[n]$, where $*$ stands for convolution and D is the equalization delay. It is convenient to develop a block formulation. Define vectors $\mathbf{g}_m := [g_m[0], \dots, g_m[L_g]]^T$, $\mathbf{g} := [\mathbf{g}_1^T, \dots, \mathbf{g}_M^T]^T$, and let \mathbf{Y}_m be a $K_f P_{ds} \times (L_g + 1)$ Toeplitz matrix with $[\mathbf{Y}_m]_{p,q} = y_m[p - q + D]$. Actually, \mathbf{Y}_m is the convolution matrix corresponding to \mathbf{y}_m . The estimate for \mathbf{z} can then be expressed as: $\hat{\mathbf{z}} = \sum_{m=1}^M \mathbf{Y}_m \mathbf{g}_m = \mathbf{Y} \mathbf{g}$, where $\mathbf{Y} := [\mathbf{Y}_1, \dots, \mathbf{Y}_M]$.

Define the $(L + L_g + 1) \times (L_g + 1)$ Toeplitz matrix \mathcal{H}_m having the $(p + 1, q + 1)$ st entry

$$[\mathcal{H}_m]_{p,q} = h_m[p - q] \quad (7)$$

from which we construct

$$\mathcal{H} := [\mathcal{H}_1, \dots, \mathcal{H}_M]. \quad (8)$$

Hence, \mathcal{H} has dimensionality

$$(L + L_g + 1) \times M(L_g + 1). \quad (9)$$

Define \mathbf{Z} as the $K_f P_{ds} \times (L + L_g + 1)$ Toeplitz matrix with $[\mathbf{Z}]_{p,q} = z[p - q + D]$. Since each column of \mathbf{Y}_m is a linear convolution of \mathbf{z} with the channel \mathbf{h}_m , we can verify that $\mathbf{Y}_m = \mathbf{Z} \mathcal{H}_m + \mathbf{E}_m$ and $\mathbf{Y} = \mathbf{Z} \mathcal{H} + \mathbf{E}$, where \mathbf{E}_m and \mathbf{E} are defined similar to \mathbf{Y}_m and \mathbf{Y} . Therefore, we arrive at

$$\hat{\mathbf{z}} = \mathbf{Y} \mathbf{g} = \mathbf{Z} \mathcal{H} \mathbf{g} + \mathbf{E} \mathbf{g}. \quad (10)$$

Notice that \mathbf{z} is the $(D + 1)$ st column of \mathbf{Z} , and thus $\mathbf{z} = \mathbf{Z} \mathbf{i}_D$, where \mathbf{i}_D denotes the $(L + L_g + 1) \times 1$ unit vector with one in its $(D + 1)$ st entry. By definition, the ZF chip equalizer must satisfy $\mathcal{H} \mathbf{g}^{\text{ZF}} = \mathbf{i}_D$. The latter indicates that the right pseudoinverse \mathcal{H}^\dagger exists: $\mathcal{H} \mathcal{H}^\dagger = \mathbf{I}_{L+L_g+1}$, and \mathbf{g}^{ZF} is just the $(D + 1)$ st column of \mathcal{H}^\dagger . Notice that the existence of \mathcal{H}^\dagger requires that \mathcal{H} is either square or fat; $(L + L_g + 1) \leq M(L_g + 1)$, which necessitates multichannel reception for ZF equalizers.

For nonsquare \mathcal{H} , the ZF equalizer \mathbf{g}^{ZF} is not unique. The minimum-norm ZF equalizer offers a unique choice that leads to the least noise enhancement

$$\mathbf{g}^{\text{ZF}} = \arg \min_{\mathbf{g}} E\{\|\mathbf{E} \mathbf{g}\|^2\}, \text{ subject to } \mathcal{H} \mathbf{g} = \mathbf{i}_D. \quad (11)$$

By solving the constrained optimization problem in (11) with the Lagrangian method, the ZF equalizer is found to be

$$\mathbf{g}^{\text{ZF}} = \mathbf{R}_E^{-1} \mathcal{H}^H (\mathcal{H} \mathbf{R}_E^{-1} \mathcal{H}^H)^{-1} \mathbf{i}_D \quad (12)$$

where $\mathbf{R}_E := E\{\mathbf{E}^H \mathbf{E}\}$. A detailed derivation for solving the same constrained optimization problem at the *chip* level can be found in [9]; the difference here is just the *frame* (or block) formulation.

The MMSE chip equalizer, on the other hand, can be found by solving the unconstrained optimization problem

$$\begin{aligned} \mathbf{g}^{\text{MMSE}} &= \arg \min_{\mathbf{g}} E\{\|\mathbf{Z} \mathcal{H} \mathbf{g} + \mathbf{E} \mathbf{g} - \mathbf{z}\|^2\} \\ &= (\mathcal{H}^H \mathbf{R}_Z \mathcal{H} + \mathbf{R}_E)^{-1} \mathcal{H}^H \mathbf{R}_Z \mathbf{i}_D \end{aligned} \quad (13)$$

where $\mathbf{R}_Z := E\{\mathbf{Z}^H \mathbf{Z}\}$. Using the matrix inversion lemma $(\mathbf{A} + \mathbf{B} \mathbf{C} \mathbf{D})^{-1} = \mathbf{A}^{-1} - \mathbf{A}^{-1} \mathbf{B} (\mathbf{D} \mathbf{A}^{-1} \mathbf{B} + \mathbf{C}^{-1})^{-1} \mathbf{D} \mathbf{A}^{-1}$, we can rewrite (13) as

$$\mathbf{g}^{\text{MMSE}} = \mathbf{R}_E^{-1} \mathcal{H}^H (\mathcal{H} \mathbf{R}_E^{-1} \mathcal{H}^H + \mathbf{R}_Z^{-1})^{-1} \mathbf{i}_D \quad (14)$$

which requires inverting a matrix of size $(L + L_g + 1)$, instead of size $M(L_g + 1)$, given that \mathbf{R}_E^{-1} is known. As usual, (14) also reveals that \mathbf{g}^{MMSE} reduces to \mathbf{g}^{ZF} at high SNR, if both exist.

Equations (12) and (14) provide general ZF and MMSE chip equalizers based on a frame of N_f chips. These equalizers are applicable even when the noise has arbitrary color. In Section IV, we will incorporate the intercell interference and simplify the equalizers accordingly.

C. Downlink CIBS-CDMA With MUI-Free Receiver

As in DS-CDMA, users in CIBS-CDMA are assigned orthonormal signature codes \mathbf{c}_u of length P_{cibs} and with each chip having amplitude $1/\sqrt{P_{\text{cibs}}}$. Distinct from conventional *symbol*

spreading, CIBS-CDMA relies on *block* spreading. Specifically, in each frame, the transmitter parses the symbol block \mathbf{s}_u into N_{sb} smaller blocks: $\mathbf{s}_u := [\tilde{\mathbf{s}}_u^T[0], \dots, \tilde{\mathbf{s}}_u^T[N_{sb}-1]]^T$. Each sub-block $\tilde{\mathbf{s}}_u[i]$ has length $K = K_f/N_{sb}$, and it is *block* spread by a tall matrix $\tilde{\mathbf{C}}_u[i]$ to obtain a chip vector $\tilde{\mathbf{C}}_u[i]\tilde{\mathbf{s}}_u[i]$. The block spreading matrix $\tilde{\mathbf{C}}_u[i]$ is designed as (see also [23] for further details when the scrambling code is absent)

$$\tilde{\mathbf{C}}_u[i] = \tilde{\mathbf{D}}_u[i]\mathbf{T}_K, \text{ with } \tilde{\mathbf{D}}_u[i] = (\tilde{\mathbf{\Delta}}[i]\mathbf{c}_u) \otimes \mathbf{I}_{K+L} \quad (15)$$

where $\mathbf{T}_K := [\mathbf{I}_K, \mathbf{0}_{K \times L}]^T$ describes again a guard-inserting² operation, and $\tilde{\mathbf{\Delta}}[i]$ is a $P_{\text{cibs}} \times P_{\text{cibs}}$ diagonal matrix holding on its diagonal the scrambling code with each chip having unit amplitude. Notice that here the scrambling code is applied in a *subblock* by *subblock* fashion, rather than a *symbol* by *symbol* fashion, as in DS-CDMA. The block spreading enabled by $\tilde{\mathbf{C}}_u[i]$ can be easily implemented by conventional symbol spreading of K symbols with $\tilde{\mathbf{\Delta}}[i]\mathbf{c}_u$, followed by a redundant chip interleaver as detailed in [23, Fig. 4]. From (15), the chip block $\tilde{\mathbf{C}}_u[i]\tilde{\mathbf{s}}_u[i]$ has length $(K+L)P_{\text{cibs}}$. As depicted in the lower part of Fig. 1, the chip vectors $\{\tilde{\mathbf{C}}_u[i]\tilde{\mathbf{s}}_u[i]\}_{i=0}^{N_{sb}-1}$ are concatenated to form the chip vector \mathbf{x}_u and, subsequently, the multiuser chip sequence \mathbf{x} in (1). For each frame containing $N_f = N_{sb}(K+L)P_{\text{cibs}}$ chips, we thus have

$$\mathbf{C}_u = \text{diag}(\tilde{\mathbf{C}}_u[0], \dots, \tilde{\mathbf{C}}_u[N_{sb}-1]). \quad (16)$$

At the receiver, we chop the received vector \mathbf{y}_m into N_{sb} pieces: $\mathbf{y}_m := [\tilde{\mathbf{y}}_m^T[0], \dots, \tilde{\mathbf{y}}_m^T[N_{sb}-1]]^T$. The i th transmitted chip vector $\tilde{\mathbf{x}}[i] = \sum_{u=1}^U A_u \tilde{\mathbf{C}}_u[i]\tilde{\mathbf{s}}_u[i]$ has the last L entries equal to zero by design [cf. (15)], which guards against interference from adjacent subblocks. Thus, $\tilde{\mathbf{y}}_m[i]$ contains contributions only from the i th information subblocks $\{\tilde{\mathbf{s}}_u[i]\}_{u=1}^U$. Based on this fact, we next focus on subblock by subblock processing. We can view $\tilde{\mathbf{x}}[i]$ as a short frame of length $\tilde{N}_f = (K+L)P_{\text{cibs}}$, with carefully designed guard intervals. This allows us to obtain [cf. (3)]

$$\tilde{\mathbf{y}}_m[i] = \tilde{\mathbf{H}}_m \tilde{\mathbf{x}}[i] + \tilde{\mathbf{e}}_m[i] \quad (17)$$

where $\tilde{\mathbf{H}}_m$ is defined similar to \mathbf{H}_m with $[\tilde{\mathbf{H}}_m]_{p,q} = h_m[p-q]$ but with size $\tilde{N}_f \times \tilde{N}_f$.

Using (15), we obtain from [23] that $\tilde{\mathbf{C}}_u[i]$ lies in the column space of $\tilde{\mathbf{D}}_u[i]$ after propagation through a frequency-selective channel: $\tilde{\mathbf{H}}_m \tilde{\mathbf{C}}_u[i] = \tilde{\mathbf{D}}_u[i]\tilde{\mathbf{H}}_m$, where $\tilde{\mathbf{H}}_m$ is a $(K+L) \times K$ Toeplitz matrix having $(p+1, q+1)$ st entry

$$[\tilde{\mathbf{H}}_m]_{p,q} = h_m[p-q]. \quad (18)$$

²For mathematical convenience, we focus, in this paper, on guard intervals formed by zeros. Alternatively, the guard interval can be filled with nonzero known symbols, as proposed in [23] and [14]. At the receiver, the contributions from known symbols are first subtracted from the received samples, and then the proposed CIBS-CDMA receiver is applied on the resulting chip sequence. The inserted known symbols can be judiciously designed to assist the receiver at the demodulation stage, as studied in [14]. Instead of zero padding, cyclic prefix extension is also possible for the CIBS-CDMA transceiver which further reduces the transceiver complexity since the MMSE block equalization reduces to a frequency domain equalization [23].

Hence, we can rewrite (17) as

$$\begin{aligned} \tilde{\mathbf{y}}_m[i] &= \tilde{\mathbf{H}}_m \sum_{u=1}^U \left(A_u \tilde{\mathbf{C}}_u[i]\tilde{\mathbf{s}}_u[i] \right) + \tilde{\mathbf{e}}_m[i] \\ &= \sum_{u=1}^U A_u \tilde{\mathbf{D}}_u[i]\tilde{\mathbf{H}}_m \tilde{\mathbf{s}}_u[i] + \tilde{\mathbf{e}}_m[i]. \end{aligned} \quad (19)$$

Exploiting the fact that $\tilde{\mathbf{D}}_u[i]$ maintains mutual orthogonality among users, $\tilde{\mathbf{D}}_u^H \tilde{\mathbf{D}}_{u'} = \delta[u-u']\mathbf{I}_{K+L}$ [23], the desired user μ despreads each block $\tilde{\mathbf{y}}_m[i]$ using $\tilde{\mathbf{D}}_\mu[i]$ to obtain an MUI-free output from the m th channel

$$\begin{aligned} \tilde{\mathbf{r}}_{\mu,m}[i] &:= \tilde{\mathbf{D}}_\mu^H[i]\tilde{\mathbf{y}}_m[i] \\ &= A_\mu \tilde{\mathbf{H}}_m \tilde{\mathbf{s}}_\mu[i] + \tilde{\mathbf{\eta}}_{\mu,m}[i] \end{aligned} \quad (20)$$

where $\tilde{\mathbf{\eta}}_{\mu,m}[i] := \tilde{\mathbf{D}}_\mu^H[i]\tilde{\mathbf{e}}_m[i]$. Let us collect $\{\tilde{\mathbf{r}}_{\mu,m}[i]\}_{m=1}^M$ into a single vector $\tilde{\mathbf{r}}_\mu[i] := [\tilde{\mathbf{r}}_{\mu,1}^T[i], \dots, \tilde{\mathbf{r}}_{\mu,M}^T[i]]^T$ and define

$$\tilde{\mathbf{H}} := [\tilde{\mathbf{H}}_1^T, \dots, \tilde{\mathbf{H}}_M^T]^T \quad (21)$$

which has dimensionality

$$M(K+L) \times K. \quad (22)$$

Defining $\tilde{\mathbf{\eta}}_\mu[i]$ similar to $\tilde{\mathbf{r}}_\mu[i]$, we thus have

$$\tilde{\mathbf{r}}_\mu[i] = A_\mu \tilde{\mathbf{H}} \tilde{\mathbf{s}}_\mu[i] + \tilde{\mathbf{\eta}}_\mu[i]. \quad (23)$$

We see that after despreading by $\tilde{\mathbf{D}}_\mu[i]$, the multiuser interference from the same cell is removed deterministically, without knowing the channels. Single-user channel equalization can now be performed on (23). Notice that different from DS-CDMA, multiuser separation in CIBS-CDMA is performed before channel equalization. The small size of symbol blocks makes block equalization possible. The CIBS-CDMA receiver relies on a block equalizer \mathbf{G}_μ , with dimensionality $K \times M(K+L)$, to estimate the i th symbol subblock as

$$\hat{\mathbf{s}}_\mu[i] = \mathbf{G}_\mu \tilde{\mathbf{r}}_\mu[i]. \quad (24)$$

The transceiver diagram is depicted in Fig. 3.

Assuming that $s_\mu[k]$ is white with variance σ_s^2 , we have $E\{\tilde{\mathbf{s}}_\mu[i]\tilde{\mathbf{s}}_\mu^H[i]\} = \sigma_s^2 \mathbf{I}_K$. Defining $\mathbf{R}_\eta := E\{\tilde{\mathbf{\eta}}_\mu[i]\tilde{\mathbf{\eta}}_\mu^H[i]\}$, linear ZF and MMSE block symbol equalizers can be expressed, respectively, as [8], [23]

$$\begin{aligned} \mathbf{G}_\mu^{\text{ZF}} &= \left[(A_\mu \tilde{\mathbf{H}})^H \mathbf{R}_\eta^{-1} (A_\mu \tilde{\mathbf{H}}) \right]^{-1} \\ &\quad \times (A_\mu \tilde{\mathbf{H}})^H \mathbf{R}_\eta^{-1} \end{aligned} \quad (25)$$

$$\begin{aligned} \mathbf{G}_\mu^{\text{MMSE}} &= \left[(A_\mu \tilde{\mathbf{H}})^H \mathbf{R}_\eta^{-1} (A_\mu \tilde{\mathbf{H}}) + \frac{1}{\sigma_s^2} \mathbf{I}_K \right]^{-1} \\ &\quad \times (A_\mu \tilde{\mathbf{H}})^H \mathbf{R}_\eta^{-1}. \end{aligned} \quad (26)$$

Note that the ZF equalizer $\mathbf{G}_\mu^{\text{ZF}}$ exists even when $M=1$, since the $(K+L) \times K$ channel matrix $\tilde{\mathbf{H}}_m$ by construction has full column rank K , regardless of the channel \mathbf{h}_m .

The equalization choices for (23) are quite flexible. We have only listed linear ZF and MMSE equalizers in (25) and (26).

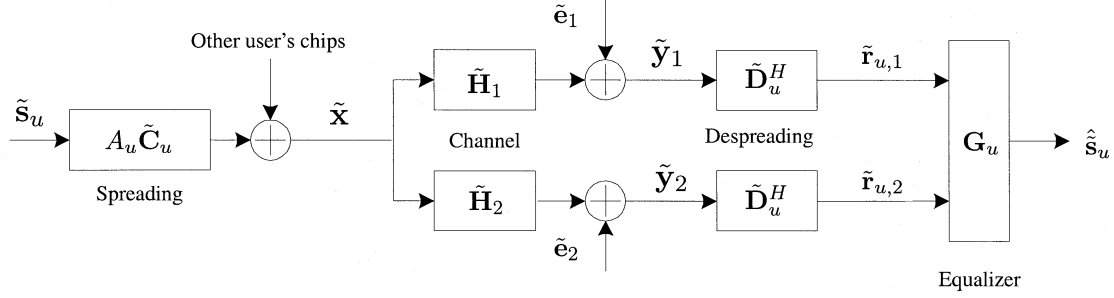


Fig. 3. Transceiver model of CIBS-CDMA.

Nonlinear equalizers, e.g., the block decision feedback equalizer (DFE) of [8] and [18], and the probabilistic data association (PDA) method of [12], are also applicable. In addition, serial equalizers can be also employed. Specifically, since $\tilde{\mathbf{r}}_{\mu,m}$ is the linear convolution of \mathbf{h}_m with $\tilde{\mathbf{s}}_\mu[i]$, treating $\tilde{\mathbf{s}}_\mu[i]$ as the chip sequence \mathbf{z} in DS-CDMA, and treating the MUI-free output $\tilde{\mathbf{r}}_{\mu,m}$ as the received sequence \mathbf{y}_m , the serial linear equalizers can be derived for CIBS-CDMA, following the same steps we took to reach (12) and (14) in Section II-B for DS-CDMA. The difference is that the serial equalizers herein operate on the symbol level, rather than the chip level. We skip the derivations of serial equalizers for brevity.

III. INTERCELL INTERFERENCE SUPPRESSION AND PERFORMANCE ANALYSIS

In this section, we analyze the intercell-interference effect that arises from nearby BSs. We assume that all BSs are synchronized, which is usually the case in a cellular configuration [5]. We further assume that the BS is located at the center of each cell. When the mobile is located at the edge of its cell, there are only a few BSs that cause significant interference. In this section, we explicitly consider one interfering BS, as in [2] and [9], but generalizations to more interfering BSs are straightforward.

Let us denote the host BS as A, and the interfering BS as B. We use $(\cdot)^a$ and $(\cdot)^b$ (or $(\cdot)_a$ and $(\cdot)_b$ when more convenient) to denote the variables associated with BSs A and B, respectively. In the presence of intercell interference, we rewrite (3) as

$$\mathbf{y}_m = \mathbf{H}_m^a \mathbf{x}^a + \mathbf{e}_m = \mathbf{H}_m^a \mathbf{x}^a + \mathbf{H}_m^b \mathbf{x}^b + \mathbf{w}_m \quad (27)$$

where \mathbf{w}_m denotes AWGN with variance $\sigma_w^2 \mathbf{I}_{N_f}$. The system model in (27) requires block synchronization for the received signals from both stations. For this purpose, the channel order L is usually overestimated as $L = \lceil (\tau_{s,\max} + T_{\text{support}} + \tau_{\text{margin}}) / T_c \rceil$, which allows the signals from the interfering BS to be τ_{margin} seconds off the signals from the desired station; i.e., the asynchronism among BSs is included as zero taps in the discrete-time equivalent channels. Notice that unlike in CIBS-CDMA, τ_{margin} is not necessary for DS-CDMA. This further suggests that CIBS-CDMA is more suitable for small cells, e.g., micro and pico cells, a typical application scenario for the TD-CDMA based UTRA TDD mode [5]. The paths from the interfering BS with delays larger than $\tau_{s,\max} + \tau_{\text{margin}}$ will be treated as additive noise. Those paths usually have negligible power, as

is the case when the mobile user is located close to the center of its cell.

Expressing the error term \mathbf{e}_m in (27) explicitly as a structured interference plus AWGN, we will be able to simplify the equalizers in Section II.

A. Downlink DS-CDMA

With $\mathbf{e}_m = \mathbf{H}_m^b \mathbf{x}^b + \mathbf{w}_m$, and \mathbf{W} defined similar to \mathbf{E} , we rewrite (10) as

$$\hat{\mathbf{z}}^a = \mathbf{Y} \mathbf{g} = \mathbf{Z}^a \mathcal{H}^a \mathbf{g} + (\mathbf{Z}^b \mathcal{H}^b + \mathbf{W}) \mathbf{g}. \quad (28)$$

Supposing that the information sequences $s_u^a[k]$ and $s_u^b[k]$ are white with variance σ_s^2 , the chip sequences $z^a[n]$ and $z^b[n]$ will also be (approximately) white with variance $\sigma_{z,a}^2 = \sum_{u=1}^{U^a} (A_u^a)^2 \sigma_s^2 / P_{ds}$, and $\sigma_{z,b}^2 = \sum_{u=1}^{U^b} (A_u^b)^2 \sigma_s^2 / P_{ds}$, respectively. The whiteness assumption of chip sequences holds because the scrambling-code chips are assumed independent and identically distributed. Notice that the number of active users U^a and U^b , as well as the power control factors for all users, affect the variances $\sigma_{z,a}^2$ and $\sigma_{z,b}^2$. We assume perfect knowledge of the channels $(\mathbf{H}_m^a, \mathbf{H}_m^b)$ and the variances $(\sigma_{z,a}^2, \sigma_{z,b}^2)$. The performance based on perfect knowledge of these parameters serves as the achievable bound for practical receivers based on estimated channels and variances.

Since $z^a[n]$, $z^b[n]$, and $\{w_m[n]\}_{m=0}^{M-1}$ are white sequences, it can be easily shown that

$$\begin{aligned} \lim_{K_f \rightarrow \infty} (K_f P_{ds})^{-1} \mathbf{R}_Z^a &= \sigma_{z,a}^2 \mathbf{I}_{L+L_g+1} \\ \lim_{K_f \rightarrow \infty} (K_f P_{ds})^{-1} \mathbf{R}_E &= \underbrace{\sigma_{z,b}^2 (\mathcal{H}^b)^H \mathcal{H}^b + \sigma_w^2 \mathbf{I}_{M(L_g+1)}}_{:=\mathbf{R}_I} \end{aligned} \quad (29)$$

where in deriving (29) we ignored the asymptotically vanishing edge effects.

Plugging (29) into (12) and (14), we obtain the chip equalizers that explicitly suppress the interference from one interfering BS

$$\begin{aligned} \mathbf{g}^{\text{ZF}} &= \mathbf{R}_I^{-1} (\mathcal{H}^a)^H \\ &\quad \times [\mathcal{H}^a \mathbf{R}_I^{-1} (\mathcal{H}^a)^H]^{-1} \mathbf{i}_D \end{aligned} \quad (30)$$

$$\begin{aligned} \mathbf{g}^{\text{MMSE}} &= \mathbf{R}_I^{-1} (\mathcal{H}^a)^H \\ &\quad \times \left[\mathcal{H}^a \mathbf{R}_I^{-1} (\mathcal{H}^a)^H + \frac{\mathbf{I}_{L+L_g+1}}{\sigma_{z,a}^2} \right]^{-1} \mathbf{i}_D. \end{aligned} \quad (31)$$

Using the matrix inversion lemma, the inverse of \mathbf{R}_I can be calculated as

$$\mathbf{R}_I^{-1} = \frac{1}{\sigma_w^2} \left\{ \mathbf{I}_{M(L_g+1)} - (\mathcal{H}^b)^H \right. \\ \left. \times \left[\mathcal{H}^b (\mathcal{H}^b)^H + \frac{\sigma_w^2}{\sigma_{z,b}^2} \mathbf{I}_{L+L_g+1} \right]^{-1} \mathcal{H}^b \right\} \quad (32)$$

which involves a matrix inversion of size $(L + L_g + 1)$ instead of $M(L_g + 1)$. When the mobile is near the center of its cell, and thus the intercell interference can be ignored, \mathbf{R}_I takes the simple form: $\mathbf{R}_I = \sigma_w^2 \mathbf{I}_{M(L_g+1)}$.

Based on a symbol-by-symbol formulation, ZF and MMSE chip equalizers were presented in [9]. We here provide alternative equalizer forms and derivations for our block formulation. By modifying the interference-plus-noise correlation matrix \mathbf{R}_I , our forms can incorporate easily multiple interfering BSs.

We next analyze the performance of the MMSE chip equalizer \mathbf{g}^{MMSE} in (31). For brevity, we denote \mathbf{g}^{MMSE} as \mathbf{g} in the ensuing derivation. After MMSE equalization, one can well approximate the residual interference-plus-noise effect as Gaussian noise [16], [21], [9]. Therefore, we can write

$$\hat{\mathbf{z}}^a = (\mathbf{Z}^a \mathcal{H}^a + \mathbf{E})\mathbf{g} = \alpha \mathbf{z}^a + \mathbf{n} \quad (33)$$

where \mathbf{n} denotes the equivalent Gaussian noise, and since $\mathbf{z}^a = \mathbf{Z}^a \mathbf{i}_D$, the scalar α is

$$\alpha = [\mathcal{H}^a \mathbf{g}]_D = \mathbf{i}_D^H \mathcal{H}^a \mathbf{g}. \quad (34)$$

The noise \mathbf{n} is colored, in general. But the entries of \mathbf{n} have identical variances, since the serial equalizer yields the same performance for each estimated chip. We are interested in this variance $\sigma_n^2 := E\{n[l]n^H[l]\} = E\{\|\mathbf{n}\|^2\}/(K_f P_{ds})$. To calculate it, we start with

$$E\{\|\hat{\mathbf{z}}^a\|^2\} = \alpha^2 E\{\|\mathbf{z}^a\|^2\} + E\{\|\mathbf{n}\|^2\}. \quad (35)$$

Using (33), (13), and (29), we obtain $E\{\|\hat{\mathbf{z}}^a\|^2\} = \mathbf{g}^H [(\mathcal{H}^a)^H \mathbf{R}_Z^a \mathcal{H}^a + \mathbf{R}_E] \mathbf{g} = \mathbf{i}_D^H \mathbf{R}_Z^a \mathcal{H}^a \mathbf{g} = K_f P_{ds} \sigma_{z,a}^2 \alpha$, and thus the noise variance is

$$\sigma_n^2 = \sigma_{z,a}^2 (\alpha - \alpha^2). \quad (36)$$

This expression will be useful in obtaining the signal to interference-plus-noise ratio (SINR) per user. Toward this objective, we plug (33) into (6) to obtain

$$\hat{s}_\mu[k] = \alpha s_\mu[k] + n_\mu[k]. \quad (37)$$

The noise $n_\mu[k]$ has variance σ_n^2/A_μ^2 , since descrambling randomizes the noise sequence \mathbf{n} , while despreading by the unit-norm user code \mathbf{c}_μ does not decrease the noise level. The SINR for each information symbol is, thus

$$\text{SINR}_\mu = \frac{A_\mu^2 \sigma_s^2}{\sigma_{z,a}^2} \frac{\alpha}{1 - \alpha}. \quad (38)$$

Notice that since α in (34) is channel dependent, so is the SINR_μ . Based on (38), the bit-error rate (BER) or the symbol

error rate (SER) can be easily calculated. For example, with BPSK signaling, the average BER is

$$P_{e,\mu} = E \left\{ \mathcal{Q} \left(\sqrt{2 \text{SINR}_\mu} \right) \right\} \quad (39)$$

where $\mathcal{Q}(\cdot)$ denotes the \mathcal{Q} function, and the averaging is taken over all channel realizations. The averaging can be carried out by Monte Carlo simulations. Thus, the performance can be predicted theoretically by (39). The validity of (39) will be confirmed in Section V. We also verified numerically that this performance result coincides with that in [9]. This is not surprising since both we and [9] start from the same assumption that the residual interference-plus-noise term can be well approximated by Gaussian noise. However, our result is neat in its simplicity.

B. Downlink CIBS-CDMA

We now analyze the structure of intercell interference in downlink CIBS-CDMA. In this subsection, we drop the subblock index i from (17) for notational convenience. Starting from (27), we first rewrite (17) as

$$\tilde{\mathbf{y}}_m = \tilde{\mathbf{H}}_m^a \sum_{u=0}^{U^a} \left(A_u^a \tilde{\mathbf{C}}_u^a \tilde{\mathbf{s}}_u^a \right) \\ + \tilde{\mathbf{H}}_m^b \sum_{v=0}^{U^b} \left(A_v^b \tilde{\mathbf{C}}_v^b \tilde{\mathbf{s}}_v^b \right) + \tilde{\mathbf{w}}_m \\ = \sum_{u=0}^{U^a} \left(A_u^a \tilde{\mathbf{D}}_u^a \tilde{\mathcal{H}}_m^a \tilde{\mathbf{s}}_u^a \right) \\ + \sum_{v=0}^{U^b} \left(A_v^b \tilde{\mathbf{D}}_v^b \tilde{\mathcal{H}}_m^b \tilde{\mathbf{s}}_v^b \right) + \tilde{\mathbf{w}}_m. \quad (40)$$

At the receiver of user μ , despreading by $\tilde{\mathbf{D}}_\mu^a$ suppresses the intracell interference. The residual intercell interference plus noise in (20) becomes

$$\tilde{\boldsymbol{\eta}}_{\mu,m} = (\tilde{\mathbf{D}}_\mu^a)^H \tilde{\mathbf{e}}_m \\ = \sum_{v=0}^{U^b} \left(A_v^b (\tilde{\mathbf{D}}_\mu^a)^H \tilde{\mathbf{D}}_v^b \tilde{\mathcal{H}}_m^b \tilde{\mathbf{s}}_v^b \right) + (\tilde{\mathbf{D}}_\mu^a)^H \tilde{\mathbf{w}}_m. \quad (41)$$

With $\rho_{\mu,v}^{a,b} = (\tilde{\boldsymbol{\Delta}}^a \mathbf{c}_\mu^a)^H (\tilde{\boldsymbol{\Delta}}^b \mathbf{c}_v^b)$ denoting the code correlation coefficient, we can verify that

$$(\tilde{\mathbf{D}}_\mu^a)^H \tilde{\mathbf{D}}_v^b = \left((\tilde{\boldsymbol{\Delta}}^a \mathbf{c}_\mu^a) \otimes \mathbf{I}_{K+L} \right)^H \left((\tilde{\boldsymbol{\Delta}}^b \mathbf{c}_v^b) \otimes \mathbf{I}_{K+L} \right) \\ = \rho_{\mu,v}^{a,b} \otimes \mathbf{I}_{K+L} \\ = \rho_{\mu,v}^{a,b} \mathbf{I}_{K+L}. \quad (42)$$

Thus, we can further simplify $\boldsymbol{\eta}_{\mu,m}$ in (41) as

$$\tilde{\boldsymbol{\eta}}_{\mu,m} = \tilde{\mathcal{H}}_m^b \sum_{v=0}^{U^b} \left(A_v^b \rho_{\mu,v}^{a,b} \tilde{\mathbf{s}}_v^b \right) + (\tilde{\mathbf{D}}_\mu^a)^H \tilde{\mathbf{w}}_m \\ := \tilde{\mathcal{H}}_m^b \tilde{\mathbf{s}}_I^b + (\tilde{\mathbf{D}}_\mu^a)^H \tilde{\mathbf{w}}_m \quad (43)$$

where $\tilde{\mathbf{s}}_I^b := \sum_{v=0}^{U^b} A_v^b \rho_{\mu,v}^{a,b} \tilde{\mathbf{s}}_v^b$ denotes the intercell interference after despreading. Since $\tilde{\boldsymbol{\Delta}}^a \mathbf{c}_\mu^a$ and $\tilde{\boldsymbol{\Delta}}^b \mathbf{c}_v^b$ are equivalent to

random codes having chips with amplitude $1/\sqrt{P_{\text{cibs}}}$, the correlation coefficient $\rho_{\mu,v}^{a,b}$ is a zero-mean random variable with variance $1/P_{\text{cibs}}$. Therefore, we have

$$\begin{aligned} E\{\hat{\mathbf{s}}_I^b(\hat{\mathbf{s}}_I^b)^H\} &= \left[\sum_{v=1}^{U^b} (A_v^b)^2 \sigma_s^2 \frac{1}{P_{\text{cibs}}} \right] \mathbf{I}_K \\ &:= \sigma_{I,b}^2 \mathbf{I}_K. \end{aligned} \quad (44)$$

Collecting $\tilde{\boldsymbol{\eta}}_\mu = [\tilde{\boldsymbol{\eta}}_{\mu,1}^T, \dots, \tilde{\boldsymbol{\eta}}_{\mu,M}^T]^T$, we obtain

$$\mathbf{R}_\eta = \sigma_{I,b}^2 \bar{\mathbf{H}}^b (\bar{\mathbf{H}}^b)^H + \sigma_w^2 \mathbf{I}_{M(K+L)}. \quad (45)$$

Applying the matrix inversion lemma, the inverse of \mathbf{R}_η can be found as

$$\begin{aligned} \mathbf{R}_\eta^{-1} &= \frac{1}{\sigma_w^2} \left\{ \mathbf{I}_{M(K+L)} - \bar{\mathbf{H}}^b \right. \\ &\quad \times \left[(\bar{\mathbf{H}}^b)^H \bar{\mathbf{H}}^b + \frac{\sigma_w^2}{\sigma_{I,b}^2} \mathbf{I}_K \right]^{-1} (\bar{\mathbf{H}}^b)^H \left. \right\} \end{aligned} \quad (46)$$

which involves a matrix inversion of size K instead of $M(K+L)$. The MMSE equalizer in (26) can then be reexpressed as

$$\begin{aligned} \mathbf{G}_\mu^{\text{MMSE}} &= \left[(A_\mu \bar{\mathbf{H}}^a)^H \mathbf{R}_\eta^{-1} (A_\mu \bar{\mathbf{H}}^a) + \frac{1}{\sigma_s^2} \mathbf{I}_K \right]^{-1} \\ &\quad \times (A_\mu \bar{\mathbf{H}}^a)^H \mathbf{R}_\eta^{-1} \end{aligned} \quad (47)$$

that copes with one interfering BS explicitly. The ZF equalizer in (25) can be similarly found. When the intercell interference is negligible, the equalizers can be further simplified by using $\mathbf{R}_\eta = \sigma_w^2 \mathbf{I}_{M(K+L)}$.

We now proceed to analyze the performance of the MMSE equalizer. Again, we replace $\mathbf{G}_\mu^{\text{MMSE}}$ by \mathbf{G}_μ , for notational brevity. The estimate for $\tilde{\mathbf{s}}_\mu$ is obtained as

$$\hat{\tilde{\mathbf{s}}}_\mu = \mathbf{G}_\mu \tilde{\mathbf{r}}_\mu = A_\mu \mathbf{G}_\mu \bar{\mathbf{H}}^a \tilde{\mathbf{s}}_\mu + \mathbf{G}_\mu \tilde{\boldsymbol{\eta}}_\mu. \quad (48)$$

The residual interference plus noise can be well approximated as additive Gaussian noise for MMSE equalizers [16], [21]. With symbol-by-symbol detection on $\hat{\tilde{\mathbf{s}}}_\mu$, (48) is equivalent to

$$\hat{s}_{\mu,k} = \alpha_{\mu,k} s_{\mu,k} + n_{\mu,k}, \quad \forall k = 0, \dots, K-1 \quad (49)$$

where $\hat{s}_{\mu,k}$ is the k th entry of $\hat{\tilde{\mathbf{s}}}_\mu$; the coefficient $\alpha_{\mu,k}$ can be expressed as $\alpha_{\mu,k} = [A_\mu \mathbf{G}_\mu \bar{\mathbf{H}}^a]_{k,k}$; and $n_{\mu,k}$ denotes the residual interference-plus-noise with variance $\sigma_s^2(\alpha_{\mu,k} - \alpha_{\mu,k}^2)$ [21]. The derivation can be also carried out following the steps in Section III-A. Therefore, the SINR for the k th symbol is

$$\text{SINR}_{\mu,k} = \frac{\alpha_{\mu,k}}{1 - \alpha_{\mu,k}}. \quad (50)$$

The average BER of the μ th user, with BPSK signaling, is

$$P_{e,\mu} = E \left\{ \frac{1}{K} \sum_{k=0}^{K-1} \mathcal{Q} \left(\sqrt{2 \text{SINR}_{\mu,k}} \right) \right\} \quad (51)$$

where the expectation is taken over random channel realizations.

Similar to the serial equalizers in DS-CDMA, serial equalizers for CIBS-CDMA can be also developed to explicitly suppress interference from one BS.

IV. SOFT HANDOFF

Soft handoff is a unique feature of CDMA systems in cellular downlink communications. Soft handoff eliminates the ping-pong effect when the mobile user is on the edge of two cells and has to switch between two BSs frequently. In the soft-handoff mode, the same information block for the desired user is transmitted simultaneously from all candidate BSs. Usually, only two BSs are involved. Let us again denote these two BSs as A and B.

A. Downlink DS-CDMA

In the soft-handoff mode, both \mathbf{z}^a and \mathbf{z}^b contain useful information for user μ . The natural approach is to demodulate the signals from these two BSs separately and then combine them optimally. This is possible using the corresponding chip equalizers that form estimates $\hat{\mathbf{z}}^a$ and $\hat{\mathbf{z}}^b$. When estimating \mathbf{z}^a , the chip equalizer treats \mathbf{z}^b as intercell interference, according to the design we detailed in Section III-A. Similarly, when estimating \mathbf{z}^b , the chip equalizer treats \mathbf{z}^a as intercell interference. Two separate symbol estimates become available

$$\hat{s}_\mu^a = \frac{1}{A_\mu^a} (\mathbf{D}_\mu^a)^H \hat{\mathbf{z}}^a, \quad \hat{s}_\mu^b = \frac{1}{A_\mu^b} (\mathbf{D}_\mu^b)^H \hat{\mathbf{z}}^b. \quad (52)$$

Notice that, in general, $A_\mu^a \neq A_\mu^b$, depending on the power controlled by each BS. For each symbol $s_\mu[k]$, we obtain from the equivalent model (37) that

$$\begin{bmatrix} \hat{s}_\mu^a[k] \\ \hat{s}_\mu^b[k] \end{bmatrix} = \begin{bmatrix} \alpha^a \\ \alpha^b \end{bmatrix} s_\mu[k] + \begin{bmatrix} n_\mu^a[k] \\ n_\mu^b[k] \end{bmatrix}. \quad (53)$$

The noise variables $n_\mu^a[k]$ and $n_\mu^b[k]$ are approximately uncorrelated, since the scrambling codes of the two BSs are random and uncorrelated. The final symbol estimate is obtained as

$$\hat{s}_\mu[k] = \lambda^a \hat{s}_\mu^a[k] + \lambda^b \hat{s}_\mu^b[k] \quad (54)$$

where the optimal weights λ^a and λ^b are determined through minimizing the MSE $E\{|\hat{s}_\mu[k] - s_\mu[k]|^2\}$. By applying the block MMSE formula (26) in the system of (53), we obtain the optimal weights as

$$\begin{bmatrix} \lambda^a \\ \lambda^b \end{bmatrix} = \frac{1}{\frac{(A_\mu^a)^2 \alpha^a}{\sigma_{z,a}^2(1-\alpha^a)} + \frac{(A_\mu^b)^2 \alpha^b}{\sigma_{z,b}^2(1-\alpha^b)} + \frac{1}{\sigma_s^2}} \begin{bmatrix} \frac{(A_\mu^a)^2}{\sigma_{z,a}^2(1-\alpha^a)} \\ \frac{(A_\mu^b)^2}{\sigma_{z,b}^2(1-\alpha^b)} \end{bmatrix}. \quad (55)$$

The postcombining SINR can be easily verified to be

$$\begin{aligned} \text{SINR}_\mu^{\text{soft}} &= \frac{(A_\mu^a)^2 \alpha^a \sigma_s^2}{\sigma_{z,a}^2(1-\alpha^a)} + \frac{(A_\mu^b)^2 \alpha^b \sigma_s^2}{\sigma_{z,b}^2(1-\alpha^b)} \\ &= \text{SINR}_\mu^a + \text{SINR}_\mu^b. \end{aligned} \quad (56)$$

Equation (56) reveals the benefit of soft handoff. The postcombining SINR is enhanced by summing the individual SINRs corresponding to two separate BSs. Since \mathcal{H}^a and \mathcal{H}^b are independent, the diversity available through these two BSs is thus collected. In contrast, a mobile in a hard-handoff mode only switches to the BS with better reception quality and, thus

$$\text{SINR}_\mu^{\text{soft}} > \text{SINR}_\mu^{\text{hard}} := \max\{\text{SINR}_\mu^a, \text{SINR}_\mu^b\}. \quad (57)$$

When two BSs have approximately identical reception quality, $\text{SINR}_\mu^a \approx \text{SINR}_\mu^b$, soft handoff offers 3-dB SINR gain over hard handoff. More importantly, soft handoff prevents the mobile from frequent switching between two BSs in such situations.

B. Downlink CIBS-CDMA

For downlink CIBS-CDMA, one can pursue the approach we detailed for DS-CDMA. That is, we first obtain $\hat{\tilde{s}}_\mu^a[z]$ and $\hat{\tilde{s}}_\mu^b[z]$, separately. The final symbol estimate is formed by optimally combining the estimated symbols from two BSs.

Instead of the aforementioned two-step approach, however, it is possible to perform a one-step detection in the CIBS-CDMA receiver. Specifically, for BS B, we have

$$\begin{aligned} \tilde{\mathbf{r}}_{\mu,m}^b &:= (\tilde{\mathbf{D}}_\mu^b)^H \tilde{\mathbf{y}}_m \\ &= A_\mu^b \tilde{\mathbf{H}}_m^b \tilde{\mathbf{s}}_\mu + \tilde{\mathbf{H}}_m^a \tilde{\mathbf{s}}_I^a + (\tilde{\mathbf{D}}_\mu^b)^H \tilde{\mathbf{w}}_m \end{aligned} \quad (58)$$

where $\tilde{\mathbf{s}}_I^a$, defined similar to $\tilde{\mathbf{s}}_I^b$, stands for the intercell interference from BS A. Collecting the outputs from M subchannels, we form $\tilde{\mathbf{r}}_\mu^a$ and $\tilde{\mathbf{r}}_\mu^b$. Next, we concatenate $\tilde{\mathbf{r}}_\mu^a$ and $\tilde{\mathbf{r}}_\mu^b$ to construct one single block $\tilde{\mathbf{r}}_\mu$ and perform block equalization once. Specifically, suppose that we have two receivers ($M = 2$), and we stack $(\tilde{\mathbf{r}}_{\mu,m}^a, \tilde{\mathbf{r}}_{\mu,m}^b)$ from different channels to obtain

$$\begin{aligned} \tilde{\mathbf{r}}_\mu &:= \begin{bmatrix} \tilde{\mathbf{r}}_{\mu,1}^a \\ \tilde{\mathbf{r}}_{\mu,2}^a \\ \tilde{\mathbf{r}}_{\mu,1}^b \\ \tilde{\mathbf{r}}_{\mu,2}^b \end{bmatrix} \\ &= \begin{bmatrix} A_\mu^a \tilde{\mathbf{H}}_1^a & \tilde{\mathbf{H}}_1^b & \mathbf{0} \\ A_\mu^a \tilde{\mathbf{H}}_2^a & \tilde{\mathbf{H}}_2^b & \mathbf{0} \\ A_\mu^b \tilde{\mathbf{H}}_1^b & \mathbf{0} & \tilde{\mathbf{H}}_1^a \\ A_\mu^b \tilde{\mathbf{H}}_2^b & \mathbf{0} & \tilde{\mathbf{H}}_2^a \end{bmatrix} \begin{bmatrix} \tilde{\mathbf{s}}_\mu \\ \tilde{\mathbf{s}}_I^a \\ \tilde{\mathbf{s}}_I^b \end{bmatrix} \\ &\quad + \begin{bmatrix} (\tilde{\mathbf{D}}_\mu^a)^H \tilde{\mathbf{w}}_1 \\ (\tilde{\mathbf{D}}_\mu^a)^H \tilde{\mathbf{w}}_2 \\ (\tilde{\mathbf{D}}_\mu^b)^H \tilde{\mathbf{w}}_1 \\ (\tilde{\mathbf{D}}_\mu^b)^H \tilde{\mathbf{w}}_2 \end{bmatrix}. \end{aligned} \quad (59)$$

If the noise vectors $\tilde{\mathbf{w}}_1, \tilde{\mathbf{w}}_2$ are independent and white Gaussian, the processed additive noise is still white Gaussian, provided that the scrambling codes from different cells are uncorrelated

$$E\{(\tilde{\mathbf{D}}_\mu^a)^H \tilde{\mathbf{D}}_\mu^b\} = E\{(\tilde{\Delta}^a \mathbf{c}_\mu^a)^H (\tilde{\Delta}^b \mathbf{c}_\mu^b)\} \mathbf{I}_{K+L} = \mathbf{0}. \quad (60)$$

In this case, we rewrite (59) as

$$\tilde{\mathbf{r}}_\mu = \begin{bmatrix} A_\mu^a \tilde{\mathbf{H}}^a \\ A_\mu^b \tilde{\mathbf{H}}^b \end{bmatrix} \tilde{\mathbf{s}}_\mu + \begin{bmatrix} \tilde{\mathbf{H}}^b \tilde{\mathbf{s}}_I^a \\ \tilde{\mathbf{H}}^a \tilde{\mathbf{s}}_I^b \end{bmatrix} + \text{AWGN}. \quad (61)$$

Based on the similarity of (61) with (23), we can now apply the block MMSE equalizers provided in (25) and (26). The correlation between $\tilde{\mathbf{s}}_I^a$ and $\tilde{\mathbf{s}}_I^b$ is on the order of $\mathcal{O}(1/P_{\text{cibs}})$, thus negligible. The correlation matrix accounting for the interference-plus-noise now becomes

$$\mathbf{R}_\eta = \text{diag}(\mathbf{R}_\eta^a, \mathbf{R}_\eta^b) \quad (62)$$

where \mathbf{R}_η^a and \mathbf{R}_η^b correspond to the correlation matrices in the two-step approach. Thus, the inverse of \mathbf{R}_η can be performed in a block diagonal fashion, $\mathbf{R}_\eta^{-1} = \text{diag}((\mathbf{R}_\eta^a)^{-1}, (\mathbf{R}_\eta^b)^{-1})$, with each block matrix inversion expressed as in (46). Thus, only matrix inversion of size K is involved, and no complexity increase occurs relative to the aforementioned two-step approach.

The joint one-step approach outperforms the suboptimum two-step approach. Notice that in the one-step approach, (61) is an overdetermined system with $2M(K+L)$ (which equals $4(K+L)$ when $M=2$) equations and only $3K$ unknowns in the absence of noise. In contrast, for the two-step approach, individual block equalization is based on $M(K+L)$ equations containing $2K$ unknowns. Notice that the one-step approach is not possible for DS-CDMA, since the two chip sequences \mathbf{z}^a and \mathbf{z}^b are different even though they include the same symbol information for the soft-handoff user.

We dealt with joint combining based on block equalizers. We remark that joint combining using serial equalizers is also possible and operates equivalently on $2M$ subchannels as in (61). Soft handoff, thus, doubles the number of equivalent subchannels in CIBS-CDMA, by exploiting the BS-induced diversity.

V. FURTHER COMPARISONS

In this section, we compare downlink CIBS-CDMA against DS-CDMA with chip equalization, from additional perspectives.

A. Maximum Intracell User Load

For each frame of fixed length N_f , we have $N_f = K_f P_{ds} + N_{\text{guard}} = N_{sb}(K_f/N_{sb} + L)P_{\text{cibs}}$; hence

$$P_{ds} \approx \left(1 + N_{sb} \frac{L}{K_f}\right) P_{\text{cibs}} = \left(1 + \frac{L}{K}\right) P_{\text{cibs}} > P_{\text{cibs}}. \quad (63)$$

The maximum achievable intracell user load is given by the spreading-code length. The fact that $P_{ds} > P_{\text{cibs}}$ indicates that DS-CDMA can afford a higher maximum intracell user load than CIBS-CDMA. This is the price paid by CIBS-CDMA for MUI-free reception within each cell due to the redundancy introduced by guard intervals. When L is small or moderate, one can choose $K \gg L$ so that $P_{ds} \approx P_{\text{cibs}}$. In this case, both systems can afford approximately the same maximum intracell user load.

It is important to underscore that the performance of CIBS-CDMA does not depend on the intracell user load U , which can change arbitrarily between 1 and P_{cibs} . On the other hand, the performance of each user in DS-CDMA degrades as the number of active users increases, since the MMSE chip equalizer can not suppress MUI perfectly, as we will demonstrate later in Section VI.

B. Receiver Complexity and Flexibility

The receiver involves three kinds of operations: equalizer design, channel equalization, and despreading. We first list the complexities for both systems using one multiply-add operation as unit:

DS-CDMA chip equalizer (complexity per symbol);
construction $2\mathcal{O}((L+L_g+1)^3)/K_f$;

TABLE I
 COMPLEXITIES OF BOTH EQUALIZERS PER INFORMATION SYMBOL

CIBS-CDMA	block equalizer	serial equalizer
construction	$2\mathcal{O}(K^3)$	$2\mathcal{O}((L + L_g + 1)^3/K_f)$
equalization	$M(K + L)$	$M(L_g + 1)$
despreading	$MP_{\text{cibs}}(1 + L/K)$	$MP_{\text{cibs}}(1 + L/K)$

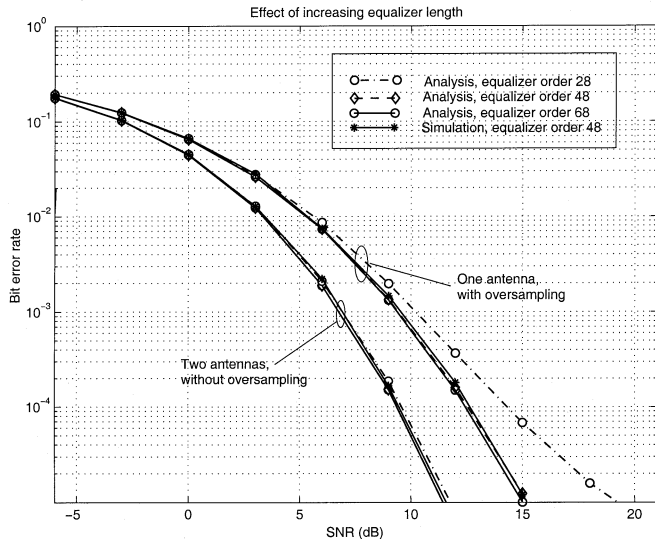


Fig. 4. Effect of chip equalizer length in DS-CDMA.

equalization $M(L_g + 1)N_f/K_f = MP_{ds}(L_g + 1)$;
 despreading $K_f P_{ds}/K_f = P_{ds}$.

CIBS-CDMA can employ both block as well as serial equalization. The complexities of both equalizers per information symbol are shown in Table I. Notice that the complexities of the equalizer designs were computed based on direct matrix inversion in (31) for DS-CDMA and in (47) for CIBS-CDMA. We underscore that low-complexity implementations are available in, e.g., [13] for DS-CDMA and [23] for CIBS-CDMA, both exploiting the Toeplitz structure of the convolutional channel matrix. For simplicity, we will not consider those alternatives in this paper.

We next compare the complexity of equalizer design for both systems, where for CIBS-CDMA we focus on block equalizers. The complexity is a cubic function of $(L + L_g + 1)$ for DS-CDMA, and of K for CIBS-CDMA. The relative complexity thus depends on the relative value of $(L + L_g + 1)$ compared with K . Suppose now we adopt the chip equalizer with $L_g = L$ (cf. Fig. 4). If we set $K = (L + L_g + 1) = 2L + 1$, both systems will have identical complexities in constructing the equalizer. In such a case, we have

$$P_{\text{cibs}} = \frac{K}{K + L} P_{ds} \approx \frac{2}{3} P_{ds}. \quad (64)$$

Therefore, CIBS-CDMA could afford lower complexity than DS-CDMA if the maximum load $P_{\text{cibs}} < (2/3)P_{ds}$; it could have higher complexity if $P_{\text{cibs}} > (2/3)P_{ds}$. Certainly, these complexities decrease quickly as the channel length decreases.

Let us now turn our attention to the complexity of equalization plus despreading. For DS-CDMA, the complexity is

$$MP_{ds}(L_g + 1) + P_{ds} > MP_{ds}L \quad (65)$$

while for CIBS-CDMA, the complexity is

$$M(K + L) + MP_{\text{cibs}}\left(1 + \frac{L}{K}\right) \approx M(K + L + P_{ds}). \quad (66)$$

Since $P_{ds}L > K + L + P_{ds}$ in practical setups, DS-CDMA requires higher complexity for equalization plus despreading than CIBS-CDMA. The main reason is that DS-CDMA needs to restore the entire chip sequence, which is P_{ds} times longer than the symbol sequence for the desired user. If serial equalizers with identical design complexities are deployed in both systems, it is clear that the receiver complexity in CIBS-CDMA is less than that in DS-CDMA.

On top of linear block and serial equalizers, CIBS-CDMA has additional equalization options. We point out two important nonlinear receivers that improve performance considerably by capitalizing on the finite-alphabet property of source symbols. One is the block DFE equalizer of [8], [18], and the other is the probabilistic data association (PDA) method in [12]. Remarkably, the PDA detector achieves a performance close to that of an optimal maximum likelihood (ML) detector. Both DFE and PDA receivers entail only cubic complexity $\mathcal{O}(K^3)$ per symbol block and are, thus, suitable for CIBS-CDMA with moderate block size K . On the contrary, for DS-CDMA receivers with chip equalization, only linear equalizers are feasible. Due to the lack of decoded symbols from other users, DFE and PDA receivers are not applicable in the DS-CDMA downlink.

C. Downlink Power Control

Mobile users are often uniformly distributed within each cell. Depending on their distances from the BS, faraway users experience far more power attenuation than nearby users. To balance the performance and lower the total transmission power, the BS may increase the transmission power toward faraway users and decrease transmission power toward nearby users. Power control is proven useful in cellular applications and is standardized in, e.g., IS-95. We here check the power control possibility for downlink CIBS-CDMA and DS-CDMA systems.

Since the intracell users are completely decoupled in CIBS-CDMA, increasing the transmit power of a certain user will not affect the performance of other users. Therefore, power control can be used very effectively in CIBS-CDMA. Optimal power allocation is simply done on a per user basis. However, the users in DS-CDMA are not completely decoupled, if MMSE chip equalization is used (MMSE equalizers outperform ZF counterparts [9]). Hence, the nearby users might experience overwhelming interference due to the power increase for faraway users. Optimal power allocation is thus complicated for DS-CDMA and needs to consider all users simultaneously.

VI. SIMULATED PERFORMANCE

We consider transmissions at a chip rate of $1/T_c = 3.84$ MHz, as specified in 3G systems [5]. We deploy the

typical urban (TUx) channel model in [1], which consists of 20 discrete delays over $\tau_{s,\max} = 2.14 \mu\text{s}$. The power of each path is decreasing as the delay increases. The last ten paths only occupy 8.8% of the total power for 20 paths. The delays and powers of the first ten taps can be also found in [13, Table II]. For the transmit and receive filters, we consider a root raised cosine filter with rolloff factor $\alpha = 0.22$ [5]. The linear convolution of transmit and receive filters yields a raised cosine filter, which is truncated to have nonzero support of $T_{\text{support}} = 9T_c$. We set $\tau_{\text{margin}} = 2.8 \mu\text{s}$. If intercell interference is strong enough to be considered, the signals from the interfering BS arrive with an arbitrary delay drawn from $[0, \tau_{\text{margin}}]$, relative to that from the desired BS. This τ_{margin} allows the interfering signals from different BSs to differ up to 0.84km when reaching the desired mobile. Correspondingly, we have $L = \lceil (\tau_{s,\max} + \tau_{\text{margin}} + T_{\text{support}}) / T_c \rceil = 28$.

We set the frame interval $T_f = 10/15 = 2/3$ ms, corresponding to one time slot in the UTRA TDD mode [5] so that each frame contains $T_f/T_c = 2560$ chips. For convenience, we set the last six chips per frame to be zero and take $N_f = 2544$. For DS-CDMA, we set the spreading gain $P_{ds} = 16$, and a guard interval of length $N_{\text{guard}} = 48$ per frame. In each frame, $K_f = 156$ symbols are transmitted per user so that $N_f = K_f P_{ds} + N_{\text{guard}}$. Correspondingly, for CIBS-CDMA, we set $P_{\text{cibs}} = 12$, $N_{sb} = 2$, $K = K_f/N_{sb} = 78$. Length 16 and length 12 Walsh Hadamard codes are deployed as user codes in DS-CDMA and CIBS-CDMA, respectively; Walsh Hadamard codes with length N exist only when $N/4$ is an integer. Complex QPSK sequences with unit amplitude are used as scrambling codes for both systems. Each user in both DS-CDMA and CIBS-CDMA systems achieves a data rate of 234 ks/s, since 156 symbols are transmitted per $2/3$ ms. However, due to the efficiency loss incurred by the guard interval, the maximum possible number of users in CIBS-CDMA is 12, which is 4 less than that of DS-CDMA; this is the price paid by CIBS-CDMA for MUI-free reception.

We plot our simulation results using two different formats. The first format fixes the number of users and evaluates performance by varying the noise power. For DS-CDMA, two typical user numbers are chosen: $U = 6$ for a medium system load and $U = 12$ for a high system load. While in CIBS-CDMA, each user's performance is not affected by the system load, and thus U can take an arbitrary value in $\{1, \dots, 12\}$. The second format fixes the noise power and compares these two systems by changing the number of users. In all simulations, we adopt BPSK signaling and define the signal to noise ratio as $\text{SNR} := \sigma_s^2 / \sigma_w^2$. Except for the power control scenario of test case 5, we fix $A_u = 1, \forall u \in \{1, \dots, U\}$. Simulation results are averaged over 1000 channels.

Test Case 1 (Equalizer Choices): We first consider a single cell system and investigate the performance of different equalizers. We consider a serial MMSE chip equalizer with order L_g for DS-CDMA and fix the delay to $D = \lfloor (L_g + L + 1) / 2 \rfloor$; the performance of the MMSE chip equalizer is insensitive to the choice of D [9]. The performance of DS-CDMA depends on the equalizer order, as demonstrated in Fig. 4 with $L_g = 28, 48, 68$. Since $L_g = 48$ is sufficient, we will adopt this choice in our following plots for DS-CDMA. Fig. 4 also verifies that brute-force

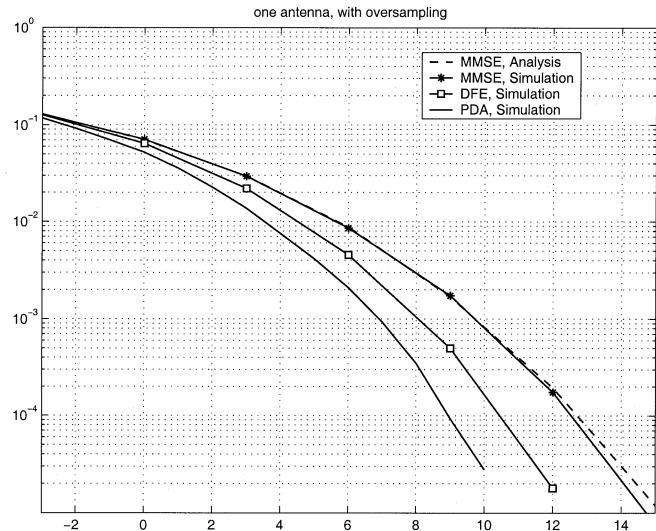


Fig. 5. Equalizer options in CIBS-CDMA.

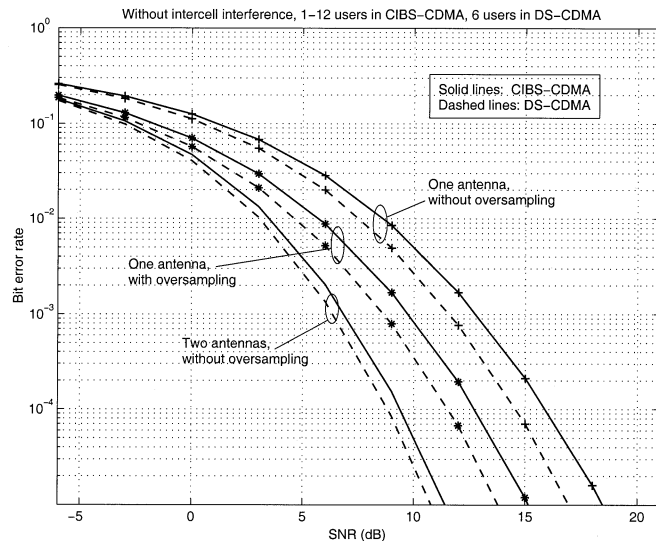


Fig. 6. BER versus SNR, 1-12 users in CIBS-CDMA, six users in DS-CDMA.

simulation results agree with the theoretical results of (38) and (39) for DS-CDMA with MMSE chip equalizers.

For CIBS-CDMA, we consider MMSE, DFE, and PDA receivers. Fig. 5 first verifies (49) and (51) for CIBS-CDMA with block MMSE equalizers. More important, it demonstrates that nonlinear PDA and DFE receivers outperform the linear MMSE equalizer considerably. Keeping this fact in mind, we next compare the performance of CIBS-CDMA against DS-CDMA, mainly using linear MMSE equalizers.

Test Case 2 (Without Intercell Interference): We assume that the desired user is located close to its BS, and the intercell interference is negligible. Figs. 6 and 7 compare the performance of CIBS-CDMA against DS-CDMA under different system loads. With linear receivers, DS-CDMA outperforms CIBS-CDMA with medium load, and both systems have comparable performance with high load. Oversampling ($M_r = 1, M_s = 2$) yields correlated channels, and the performance is noticeably worse than that with two receive antennas ($M_r = 2, M_s = 1$).

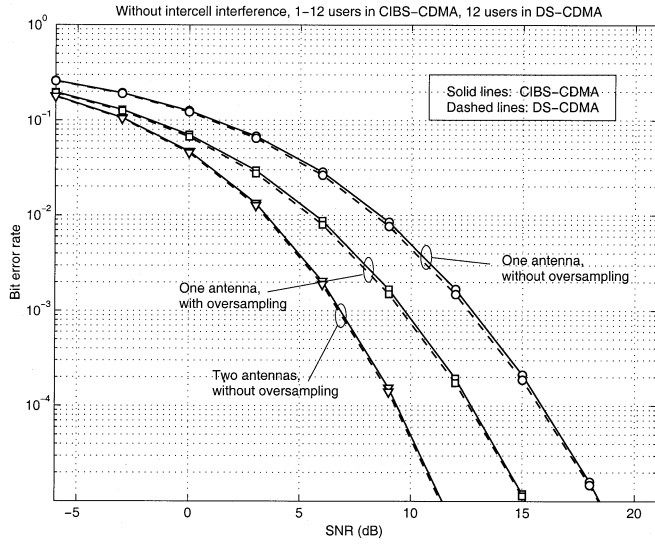


Fig. 7. BER versus SNR, 1-12 users in CIBS-CDMA, 12 users in DS-CDMA.

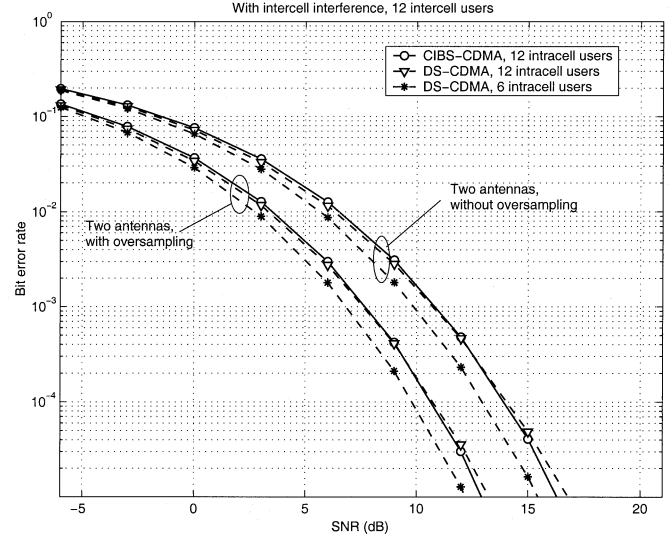


Fig. 9. With intercell interference, 12 intercell users.

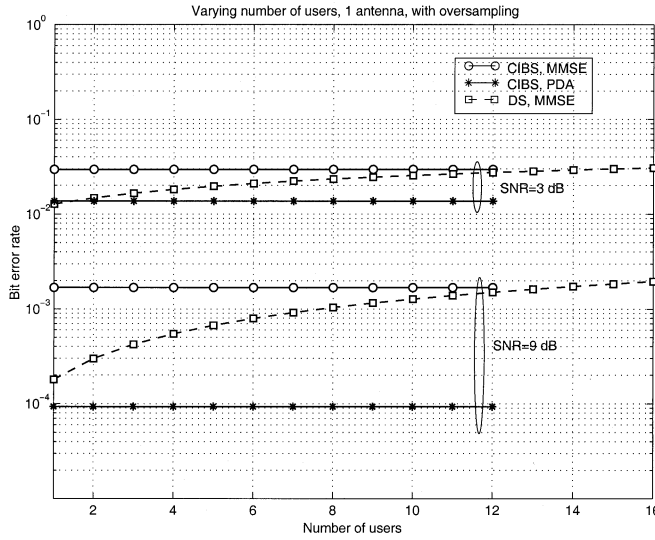


Fig. 8. BER versus the number of users (no intercell interference).

Fig. 8 plots the BER performance with varying number of users at SNR = 3 dB, and SNR = 9 dB. At all system loads, DS-CDMA outperforms CIBS-CDMA with linear receivers, yet is inferior to CIBS-CDMA with nonlinear PDA receivers. Thanks to the cubic complexity $\mathcal{O}(K^3)$, the PDA receiver turns out to be an attractive choice for CIBS-CDMA.

Test Case 3 (With Intercell Interference): The desired user is now located on the edge of its cell. We assume that the channels corresponding to the interfering BS have the same average power as those of the desired BS. We deploy linear MMSE receivers with two receive antennas and assume that the interfering cell has 12 active users. Fig. 9 reveals similar results as in Figs. 6 and 7.

Test Case 4 (Soft Handoff): We assume that the desired user is located on the edge of two cells, and soft handoff is invoked. Since the number of active users in one cell determines the interference power to the other cell, the performance of both systems under soft handoff depends on the number of active users

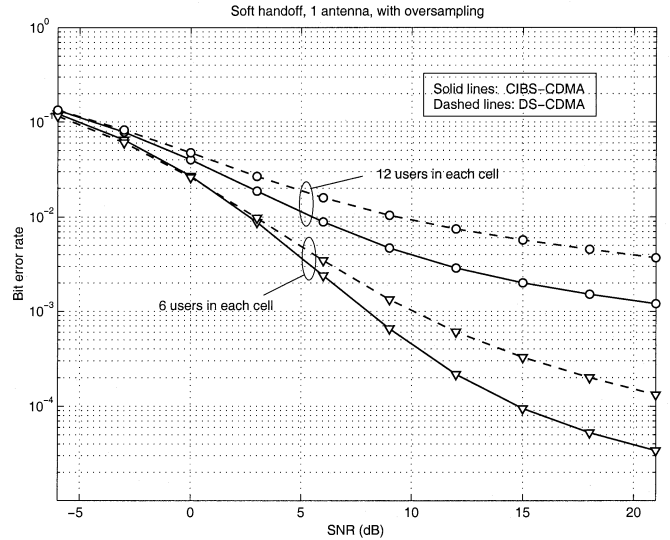


Fig. 10. Soft handoff, one antenna with oversampling.

in both cells. We set $U^a = U^b$ and compare the performance of CIBS-CDMA and DS-CDMA in Figs. 10 and 11, with one and two receive antennas, respectively. Even with linear receivers, we infer from Fig. 10 that CIBS-CDMA has a clear advantage over DS-CDMA in soft handoff with one receive antenna, thanks to the one-step approach in (59). This advantage decreases when two receive antennas and oversampling ($M = 4$) are used, as shown in Fig. 11.

Fig. 12 plots the BER performance with varying number of users in the soft handoff mode at SNR = 9 dB. When the system load increases, CIBS-CDMA outperforms DS-CDMA.

Test Case 5 (Downlink Power Control): We now test downlink power control and omit intercell interference for brevity. We divide users into three groups, each having $A_u = 2, 1, 1/2$, respectively. Hence, strong users have 6 dB of u more power than normal users, and normal users have 6 dB more power over weak users (here, “strong,” “normal,” and “weak” refer to the relative transmitted powers among users). With one antenna and

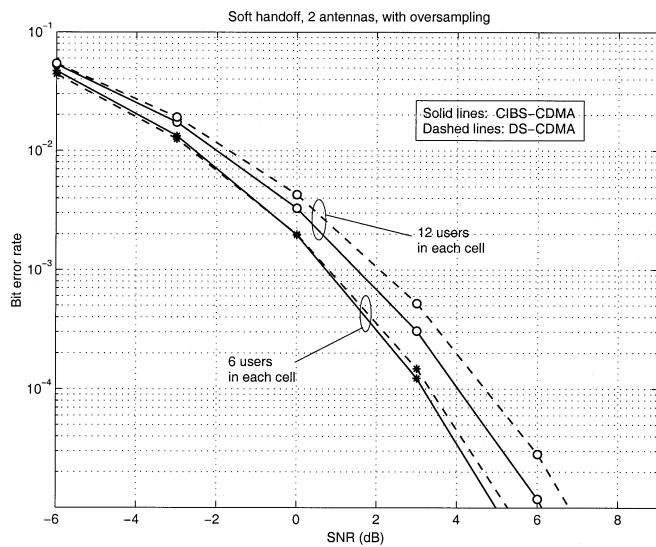


Fig. 11. Soft handoff, two antennas with oversampling.

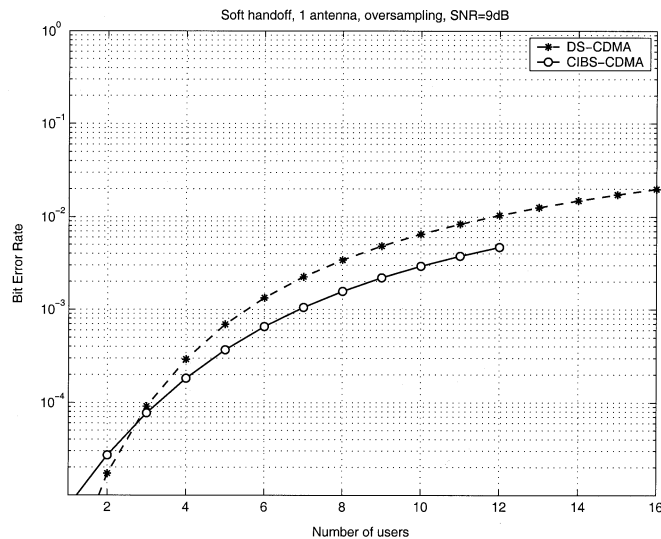


Fig. 12. Soft handoff, BER versus the number of users.

oversampling ($M_r = 1, M_s = 2$), Figs. 13 and 14 show the performance with six and 12 users, respectively. Notice that each user's performance in CIBS-CDMA is independent of other users; thus, an exact 6-dB performance difference appears according to the 6-dB transmit-power differences among users. On the other hand, the performance gap for different users is more pronounced than the transmit-power differences in DS-CDMA. We clearly see that weak users suffer from the boosted power of strong users.

VII. CONCLUSION

In this paper, we compared the recently proposed CIBS-CDMA against the conventional DS-CDMA in a wireless cellular downlink configuration. We provided a unifying model for both systems and investigated their performance in the presence of intercell interference and soft handoff. Extensive comparisons from load, performance, complexity,

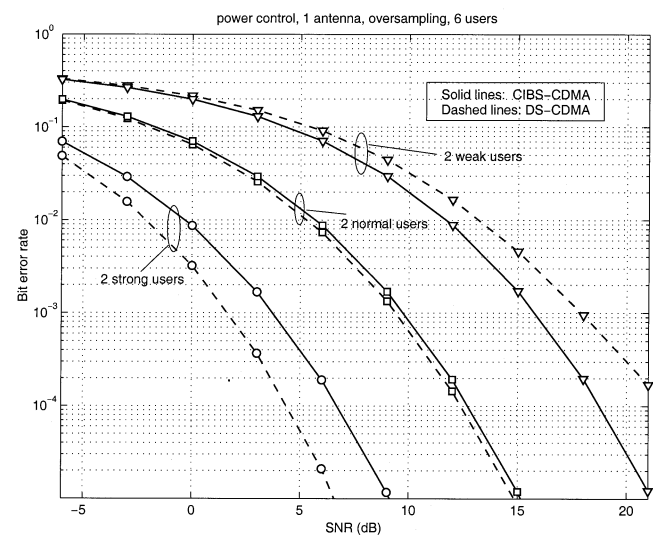


Fig. 13. Power control, one antenna, with oversampling, six users.

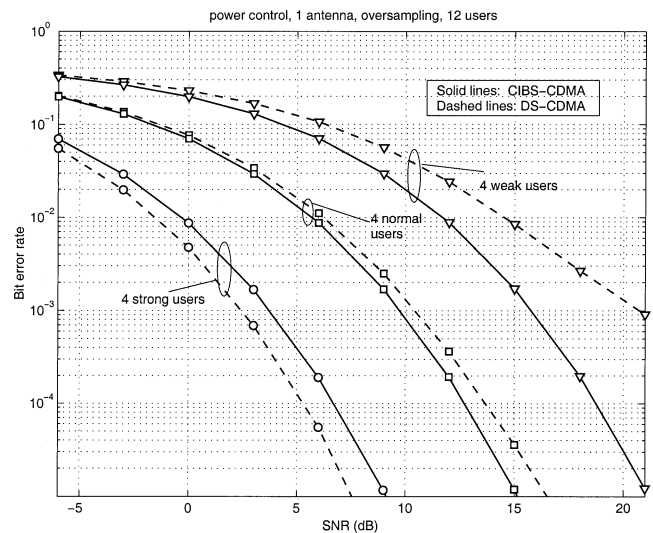


Fig. 14. Power control, one antenna, with oversampling, 12 users.

and flexibility perspectives illustrate the merits, along with the disadvantages, of CIBS-CDMA over DS-CDMA and, thus, reveal its potential for future wireless systems.

We have assumed time-invariant channels per data frame and perfect channel knowledge at the receiver. Practical issues including synchronization, channel estimation, and the impact of channel variation on performance are items in our future research agenda on CIBS-CDMA.

ACKNOWLEDGMENT

The authors would like to thank one of the reviewers for clarifying the performance dependence on the chip equalizer length for DS-CDMA and all the reviewers for their helpful comments that improved the presentation of this paper.

REFERENCES

- [1] "3GPP Technical Rep.," TSG RAN WG4: Deployment Aspects, 3G TR 25.943.

- [2] C. D. Frank, E. Visotsky, and U. Madhoo, "Adaptive interference suppression for the downlink of a direct sequence CDMA system with long spreading sequences," *J. VLSI Signal Process.*, vol. 30, pp. 273–291, Mar. 2002.
- [3] I. Ghauri and D. T. M. Slock, "Linear receivers for the ds-CDMA downlink exploiting orthogonality of spreading sequences," in *Proc. Asilomar Conf. Signals, Systems, Computers*, vol. 1, Pacific Grove, CA, Nov. 1998, pp. 650–654.
- [4] G. B. Giannakis, Z. Wang, A. Scaglione, and S. Barbarossa, "AMOUR-generalized multi-carrier transceivers for blind CDMA regardless of multipath," *IEEE Trans. Commun.*, vol. 48, pp. 2064–2076, Dec. 2000.
- [5] M. Haardt, A. Klein, R. Koehn, S. Oestreich, M. Purat, V. Sommer, and T. Ulrich, "The TD-CDMA based UTRA TDD mode," *IEEE J. Select. Areas Commun.*, vol. 18, pp. 1375–1385, Aug. 2000.
- [6] K. Hooli, M. Latvaaho, and M. Juntti, "Multiple access interference suppression with linear chip equalizers in WCDMA downlink receivers," in *Proc. Global Telecommunications Conf.*, vol. 1a, Rio de Janeiro, Brazil, Dec. 1999, pp. 467–471.
- [7] A. Klein, "Data detection algorithms specially designed for the downlink of CDMA mobile radio systems," in *Proc. Vehic. Technol. Conf.*, vol. 1, Phoenix, AZ, May 1997, pp. 203–207.
- [8] A. Klein, G. K. Kaleh, and P. W. Baier, "Zero forcing and minimum mean-square-error equalization for multiuser detection in code-division multiple-access channels," *IEEE Trans. Vehic. Technol.*, vol. 45, pp. 276–287, May 1996.
- [9] T. P. Krauss, W. J. Hillery, and M. D. Zoltowski, "Downlink specific linear equalization for frequency selective CDMA cellular systems," *J. VLSI Signal Process.*, vol. 30, pp. 143–161, Mar. 2002.
- [10] T. P. Krauss, M. D. Zoltowski, and G. Leus, "Simple MMSE equalizers for CDMA downlink to restore chip sequence: Comparison to zero forcing and RAKE," in *Proc. Int. Conf. ASSP*, vol. 5, Istanbul, Turkey, June 2000, pp. 2865–2868.
- [11] G. Leus and M. Moonen, "MUI-free receiver for a synchronous DS-CDMA system based on block spreading in the presence of frequency-selective fading," *IEEE Trans. Signal Process.*, vol. 48, pp. 3175–3188, Nov. 2000.
- [12] J. Luo, K. R. Pattipati, P. K. Willett, and F. Hasegawa, "Near-optimal multiuser detection in synchronous CDMA using probabilistic data association," *IEEE Commun. Lett.*, vol. 5, pp. 361–363, Sept. 2001.
- [13] L. Mailaender, "Low complexity implementation of CDMA downlink equalization," in *Proc. 3G 2001 Conf.*, U.K., Mar. 26, 2001.
- [14] F. Petre, G. Leus, L. Deneire, and M. Moonen, "Downlink frequency domain chip equalization for single carrier block transmission DS-CDMA with known symbol padding," in *Proc. GlobeCom*, Taipei, Taiwan, Nov. 2002.
- [15] F. Petre, G. Leus, M. Engels, M. Moonen, and H. De Man, "Semi-blind space-time chip equalizer receivers for WCDMA forward link with code-multiplexed pilot," in *Proc. Int. Conf. ASSP*, Salt Lake City, UT, May 2001, pp. 2245–2248.
- [16] H. V. Poor and S. Verdú, "Probability of error in MMSE multiuser detection," *IEEE Trans. Inform. Theory*, vol. 43, pp. 858–871, May 1997.
- [17] H. Sari and G. Karam, "Orthogonal frequency-division multiple access and its application to CATV network," *Eur. Trans. Telecommun.*, vol. 9, pp. 507–516, Nov./Dec. 1998.
- [18] A. Stamoulis, G. B. Giannakis, and A. Scaglione, "Block FIR decision-feedback equalizers for filterbank precoded transmissions with blind channel estimation capabilities," *IEEE Trans. Commun.*, vol. 49, pp. 69–83, Jan. 2001.
- [19] R. G. Vaughan, "Polarization diversity in mobile communications," *IEEE Trans. Vehic. Technol.*, vol. 39, pp. 177–186, Aug. 1990.
- [20] S. Verdú, *Multiuser Detection*. Cambridge, MA: Cambridge Univ. Press, 1998.
- [21] X. Wang and H. V. Poor, "Iterative (Turbo) soft interference cancellation and decoding for coded CDMA," *IEEE Trans. Commun.*, vol. 46, pp. 1046–1061, July 1999.
- [22] Z. Wang and G. B. Giannakis, "Wireless multicarrier communications: Where Fourier meets Shannon," *IEEE Signal Process. Mag.*, vol. 17, pp. 29–48, May 2000.
- [23] S. Zhou, G. B. Giannakis, and C. Le Martret, "Chip interleaved block spread code division multiple access," *IEEE Trans. Commun.*, vol. 50, pp. 235–248, Feb. 2002.



Shengli Zhou (M'03) received the B.S. and M.Sc. degrees from the University of Science and Technology of China (USTC), Hefei, China, in electrical engineering and information science, in 1995 and 1998, respectively. He received the Ph.D. degree from the Department of Electrical and Computer Engineering, University of Minnesota, Minneapolis, in 2002.

He joined the Department of Electrical and Computer Engineering, University of Connecticut, Storrs, CT, as an Assistant Professor, in 2003. His research interests include the areas of communications and signal processing, including channel estimation and equalization, multiuser and multicarrier communications, space-time coding, adaptive modulation, and cross-layer designs.



Pengfei Xia (S'03) received the B.S. and M.S. degrees in electrical engineering from the University of Science and Technology of China (USTC), Hefei, China, in 1997 and 2000, respectively. He is currently working toward the Ph.D. degree at the University of Minnesota, Minneapolis.

His research interests include the areas of signal processing and communications, including multiple-input multiple-output wireless communications, transceiver designs, adaptive modulation, multicarrier transmissions, space-time coding, and iterative decoding techniques.



Geert Leus (M'00) was born in Leuven, Belgium, in 1973. He received the electrical engineering degree and the Ph.D. degree in applied sciences from the Katholieke Universiteit Leuven, Leuven, Belgium, in 1996 and 2000, respectively.

He was a Research Assistant and a Postdoctoral Fellow of the Fund for Scientific Research—Flanders, Belgium, from October 1996 until September 2003. During that period, he was affiliated with the Electrical Engineering Department of the Katholieke Universiteit Leuven, Leuven, Belgium. Currently, he is an Assistant Professor at the Faculty of Electrical Engineering, Mathematics and Computer Science, Delft University of Technology, The Netherlands. During the summer of 1998, he visited Stanford University, and from March 2001 until May 2002 he was a Visiting Researcher and Lecturer at the University of Minnesota, Minneapolis. His research interests are in the area of signal processing for communications.

Dr. Leus received a 2002 IEEE Signal Processing Society Young Author Best Paper Award. He is a member of the IEEE Signal Processing for Communications Technical Committee and an Associate Editor for the IEEE TRANSACTIONS ON WIRELESS COMMUNICATIONS and the IEEE SIGNAL PROCESSING LETTERS.



Georgios B. Giannakis (S'84–M'86–SM91–F'97) received the Diploma in electrical engineering from the National Technical University of Athens, Athens, Greece, in 1981. He received the M.Sc. degree in electrical engineering from the University of Southern California (USC) in 1983, the MSc. degree in mathematics in 1986, and the Ph.D. degree in electrical engineering in 1986.

From September 1982 to July 1986, he was with USC. After lecturing for one year at USC, he joined the University of Virginia, Blacksburg, in 1987, where he became a Professor of electrical engineering in 1997. Since 1999, he has been a Professor with the Department of Electrical and Computer Engineering, University of Minnesota, Minneapolis, where he now holds an ADC Chair in Wireless Telecommunications. His research interests span the areas of communications and signal processing, estimation and detection theory, time-series analysis, and system identification—subjects on which he has published more than 150 journal papers, 300 conference papers, and two edited books. Current research interests focus on transmitter and receiver diversity techniques for single- and multi-user fading communication channels, precoding and space-time coding for block transmissions, multicarrier, and ultrawide-band wireless communication systems. He is a frequent consultant for the telecommunications industry.

Dr. Giannakis is the (Co-) Recipient of four best paper awards from the IEEE Signal Processing Society (1992, 1998, 2000, 2001). He also received the Society's Technical Achievement Award in 2000. He co-organized three IEEE-SP Workshops and was (Co-) Guest Editor for four special issues. He has served as Editor-in-Chief for the IEEE SIGNAL PROCESSING LETTERS, as Associate Editor of the IEEE TRANSACTIONS ON SIGNAL PROCESSING and the IEEE SIGNAL PROCESSING LETTERS, as Secretary of the SP Conference Board, as member of the SP Publications Board, as member and Vice Chair of the Statistical Signal and Array Processing Technical Committee, and as Chair of the SP for Communications Technical Committee. He is a member of the Editorial Board for the PROCEEDINGS OF THE IEEE, and the steering committee of the IEEE TRANSACTIONS ON WIRELESS COMMUNICATIONS. He is a member of the IEEE Fellows Election Committee and the IEEE-SP Society's Board of Governors.